


# Nanomaterial-Based Scaffolds for Tissue Engineering Applications: A Review on Graphene, Carbon Nanotubes and Nanocellulose

Gurshagan Kandhola<sup>1,2</sup> · Sunho Park<sup>3,4,5</sup> · Jae-Woon Lim<sup>6</sup> · Cody Chivers<sup>1,2</sup> · Young Hye Song<sup>7</sup> · Jong Hoon Chung<sup>6</sup> · Jangho Kim<sup>3,4,5</sup> · Jin-Woo Kim<sup>1,2,8</sup> 

Received: 26 October 2022 / Revised: 10 February 2023 / Accepted: 15 February 2023 / Published online: 15 April 2023  
© Korean Tissue Engineering and Regenerative Medicine Society 2023

**Abstract** Nanoscale biomaterials have garnered immense interest in the scientific community in the recent decade. This review specifically focuses on the application of three nanomaterials, i.e., graphene and its derivatives (graphene oxide, reduced graphene oxide), carbon nanotubes (CNTs) and nanocellulose (cellulose nanocrystals or CNCs and cellulose nanofibers or CNFs), in regenerating different types of tissues, including skin, cartilage, nerve, muscle and bone. Their excellent inherent (and tunable) physical, chemical, mechanical, electrical, thermal and optical properties make them suitable for a wide range of biomedical applications, including but not limited to diagnostics, therapeutics, biosensing, bioimaging, drug and gene delivery, tissue engineering and regenerative medicine. A state-of-the-art literature review of composite tissue scaffolds fabricated using these nanomaterials is provided, including the unique physicochemical properties and mechanisms that induce cell adhesion, growth, and differentiation into specific tissues. In addition, *in vitro* and *in vivo* cytotoxic effects and biodegradation behavior of these nanomaterials are presented. We also discuss challenges and gaps that still exist and need to be addressed in future research before clinical translation of these promising nanomaterials can be realized in a safe, efficacious, and economical manner.

**Keywords** Carbon nanotubes · Graphene · Cellulose nanocrystals · Cellulose nanofibers · Tissue engineering · Regenerative medicine

Gurshagan Kandhola and Sunho Park are contributed equally to this work.

✉ Jangho Kim  
rain2000@jnu.ac.kr

✉ Jin-Woo Kim  
jwkim@uark.edu

<sup>1</sup> Department of Biological and Agricultural Engineering, University of Arkansas, Fayetteville, AR, USA

<sup>2</sup> Institute for Nanoscience and Engineering, University of Arkansas, Fayetteville, AR, USA

<sup>3</sup> Department of Convergence Biosystems Engineering, Chonnam National University, Gwangju 61186, Republic of Korea

<sup>4</sup> Department of Rural and Biosystems Engineering, Chonnam National University, Gwangju 61186, Republic of Korea

<sup>5</sup> Interdisciplinary Program in IT-Bio Convergence System, Chonnam National University, Gwangju 61186, Republic of Korea

<sup>6</sup> Department of Biosystems and Biomaterials Science and Engineering, Seoul National University, Seoul 08826, Republic of Korea

<sup>7</sup> Department of Biomedical Engineering, University of Arkansas, Fayetteville, AR, USA

<sup>8</sup> Materials Science and Engineering Program, University of Arkansas, Fayetteville, AR, USA

## 1 Introduction

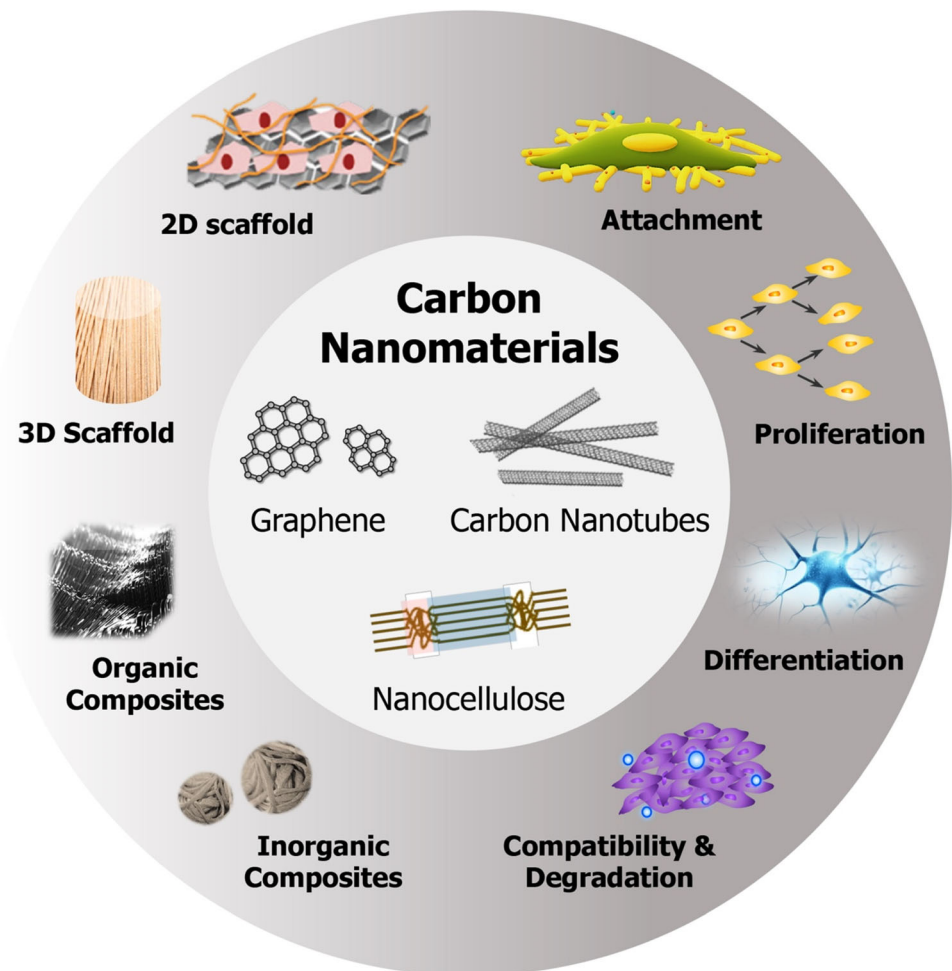
The concept of tissue engineering was developed in the early 1960s when the field of biomaterials was still nascent. As biomaterials research expanded to encompass all biocompatible materials specifically designed for use in the body, there came a need to integrate cells and biologically active molecules into these systems for them to become seamless working tissues. To achieve this level of sophistication and mimic native tissue archetypes, scaffolds need to be fabricated by interweaving biomaterials, cells, and biologically active molecules in the matrix, thus promoting cell attachment, growth, differentiation, and even migration as needed. The overarching goal of tissue engineering is the creation of biocomposites that can restore damaged tissues by (a) providing structural support to facilitate cell adhesion and new cellular growth, and (b) maintaining cell physiology and intercellular molecular signaling to facilitate new cellular growth. Restoring large sections of tissues may also lead to salvation of a complete organ. Scaffolds must provide a microenvironment suitable for adsorption of proteins and adhesion of cells. Based on the target tissue in concern, scaffold microstructures must be designed to have specific physicochemical properties, such as mechanical strength, surface chemistry and roughness, wettability, etc. to promote (a) adsorption of adhesive proteins released by surrounding cells before they attach, and (b) sustained release of a multitude of biomolecules (e.g., growth factors) incorporated into the matrix to promote cell growth and differentiation; for example, attachment of osteoblasts, followed by cellular growth and formation of new bone structures [1, 2].

Among the different materials that have potential for use in tissue engineering and regenerative medicine, significant advances have been made in the development of scaffolds using nanomaterials, such as graphene (graphene foam, graphene oxide (GO) and reduced graphene oxide (rGO)), carbon nanotubes (CNTs), fullerenes, carbon dots, nanodiamonds, and cellulose nanoparticles (cellulose nanocrystals (CNCs) and cellulose nanofibers (CNFs)) [3–5]. However, there still are major challenges that need to be addressed before successful clinical translation of these promising nanomaterials can be realized. To achieve full potential, an engineered scaffold must efficiently mimic *in vivo* characteristics of the target tissue with respect to cellular, morphological, and physiological organizations [6–9]. Tissue microenvironments comprise unique variations of cell–cell and cell–extracellular matrix (ECM) interactions as well as soluble macromolecules and defined chemical and physical cues. Scaffolds must be 3D porous, bioabsorbable, bioactive, and biocompatible structures with mechanical properties that match those of

native tissues and degradation properties that match the rate of synthesis of new ECM [10]. A well-designed tissue engineering scaffold is one that dynamically interacts with living cells for an effective repair of damaged tissue. The more common approach to fabricating scaffolds is through the bottom-up approach of material development, in which matrix surfaces are modified with specific bioactive peptides to actively elicit desired cellular responses [10, 11]. The most important factor that impacts cellular response to a scaffold is how proteins adsorb at the interface between the material and the growth medium during *in vitro* studies, or blood or tissue fluid during *in vivo* testing [10]. Several factors, including but not limited to, surface interfacial free energy, wettability, hydrophobicity/hydrophilicity, chemical functionality, surface charge, topography, and roughness, impact the mechanism and extent of protein adsorption and cell adhesion and proliferation. When designing scaffolds, aiming for mechanical, structural, and functional characteristics like those of native tissues is a mandatory prerequisite to preventing failure after implantation [10, 11]. Different tissues throughout the body are exposed to different stimuli and microenvironments, and thus require specific materials with customized physicochemical properties for successful cell growth and differentiation leading to tissue restoration [12–16]. As an example, the heart's function is to act as a pump driving the flow of blood throughout the body. Therefore, for a cardiac tissue scaffold to be practically useful and not fail *in vivo*, it must mimic the electrical and mechanical properties of the cardiac muscle. It must be conductive enough to facilitate electrical signal transduction from cell to cell while maintaining sufficient mechanical strength to withstand the continuous cyclic contractions of the heart for the remainder of the individual's life or until the tissue has been completely restored and the scaffold dissolved or otherwise removed. If the scaffolding materials have poor electrical integration, it can lead to arrhythmia and other secondary complications [17, 18].

Since their discovery, carbon-based nanomaterials such as fullerenes (1985), carbon nanotubes (1991), and graphene sheets (2004) have sparked significant interest in research fields spanning many different disciplines [19–21]. Cellulose nanocrystals, on the other hand, were discovered long ago (1949); however, their use in tissue engineering wasn't investigated until late 1990s and early 2000s. The reason behind the explosion of scientific interest in these nanomaterials lies within the unique physicochemical properties (nanoscale morphology, tunable surface chemistry, exceptional mechanical strength, and electrical conductivity) and high biocompatibility they display. These properties make them highly desirable for a variety of biomedical applications, positioning these materials as excellent candidates for cancer therapy,

**Fig. 1** Depiction of three nanomaterials, i.e., graphene, carbon nanotubes, and nanocellulose, and their roles in tissue engineering. In this review, we discuss how 2D/3D scaffolds and/or organic/inorganic nanocomposites fabricated with these nanomaterials have been used to improve cell attachment, proliferation, and differentiation into specific tissues, as well as their biocompatibility and biodegradability behaviors (adapted with permission from [5])

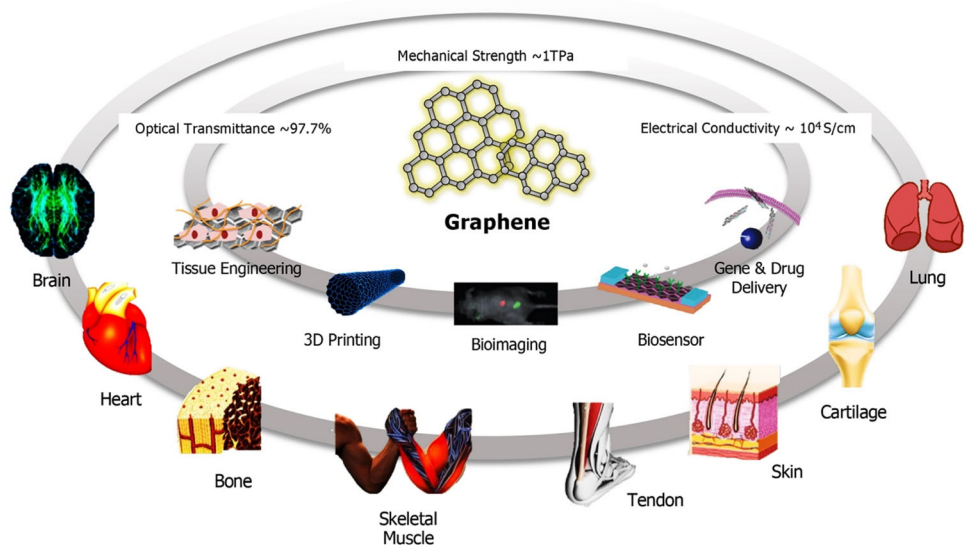


photothermal treatment, drug and gene delivery, imaging of cells and tissues, biosensing, and last but not least tissue engineering and regenerative medicine [22–27]. Incorporating nanomaterials into polymer matrices to produce composite scaffolds provides spatial and temporal control over various physiological processes involved in tissue regeneration with a high degree of precision [19]. In this review, we discuss three nanomaterials, i.e., graphene, CNTs and nanocellulose, in the context of tissue engineering with a focus on how composite scaffolds containing these nanomaterials enhance cell attachment, growth, and differentiation; in addition, cytotoxicity concerns and *in vivo* biodegradation behavior is also discussed (Fig. 1). Suggestions on how existing challenges and bottlenecks can be addressed, to realize the tremendous clinical potential of these nanoscale materials for tissue engineering applications, is presented in the summary and future perspectives section.

## 2 Graphene

Single layer graphene is an one atom thick two-dimensional (2D) material consisting of  $sp^2$  hybridized carbon atoms arranged in a honeycomb lattice structure. Few-layer graphene, on the other hand, consists of a few atomic layers (*i.e.*, 2–10 layers) held together by van der Waals forces [28]. It has been shown that  $> 10$  layers of graphene begin to act chemically as graphite [29], indicating that the intermolecular interactions between graphene sheets determine the physical characteristics observed in bulk. Graphene is one of the most important crystalline allotropes of carbon, where each carbon atom in a single layer is covalently bound to neighboring carbon atoms via three  $\sigma$ -bonds and one out-of-plane  $\pi$ -bond [30, 31]. The strong in-plane carbon–carbon bonding and the presence of free  $\pi$  electrons (two in every hexagon) and reactive sites for chemical modifications make graphene a unique material with exceptional electrical, mechanical, thermal, optical, and physicochemical properties, for example, Young’s

**Fig. 2** Schematic illustrating graphene's unique physicochemical properties, along with its highly modifiable surface chemistry and large surface areas, which make it a versatile material for engineering a variety of tissues, ranging from cardiac muscle and bones to skin and cartilage (adapted with permission from [9])



Modulus of 1 TPa, electrical conductivity of  $10^4$  S/cm, thermal conductivity of 5000 W/mK, optical transmittance of 97.7%, and large surface area ( $2630 \text{ m}^2/\text{g}$ ) [30, 32].

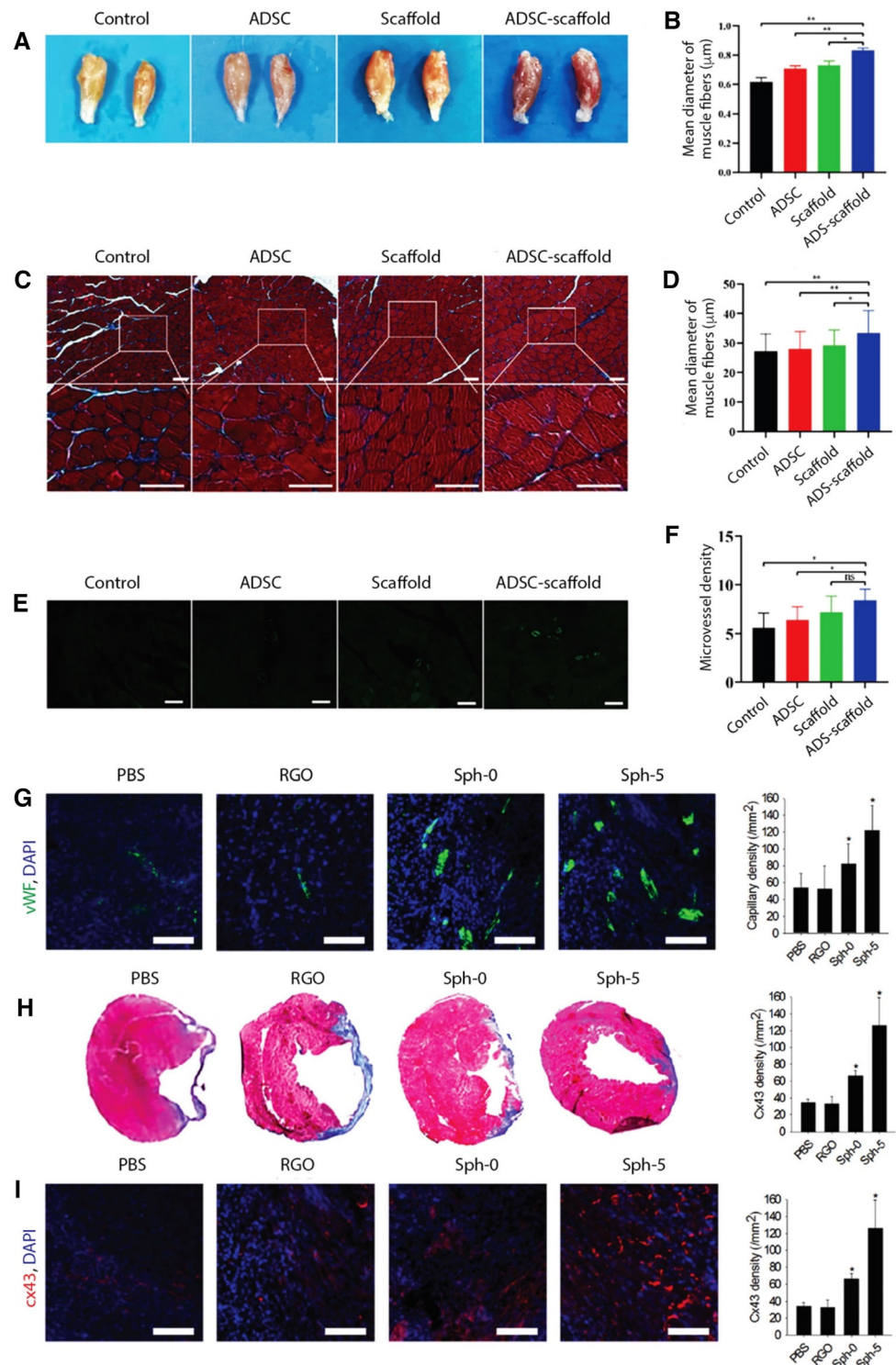
Graphene can take many forms, from graphene oxide (GO) and reduced GO (rGO) to graphene foams (GFs), differing in surface chemistry (*i.e.*, type and amount of chemical modification), purity, lateral dimensions, defect density, and composition, ultimately impacting its properties and suitability for specific applications [32, 33]. All forms of graphene have been found useful for tissue engineering; however, GO has proven to be the most valuable platform due to its dispersibility in water, colloidal stability, hydrophilicity, and ability to interface with chemical and biological molecules through surface reactions and H-bonding [32, 33]. On the other hand, graphene and rGO have a greater tendency to aggregate and cause cytotoxicity. Graphene's large surface area, highly modifiable surface chemistry, and its ability to interact and interface with cells and tissues can be exploited for biomedical applications, including drug/gene delivery, bioimaging, biosensing, theranostics, tissue engineering and regenerative medicine (Fig. 2) [9, 34]. Here, we discuss the latest literature on how graphene is being used to enhance the robustness and biocompatibility of tissue engineering scaffolds for improved cell attachment and differentiation.

## 2.1 Tissue scaffolds

Graphene and its derivatives can either be used as 2D coating materials on the surface of substrates such as glass, PDMS, and  $\text{SiO}_2/\text{Si}$ , or as additives in three-dimensional (3D) polymeric scaffolds where graphene is either coated on the surface or incorporated into a matrix to match the

properties of the scaffold with those of target tissue being reconstructed [32–34]. For instance, mesenchymal stem cells (MSCs) are highly sensitive to scaffold elasticity and modulating scaffold stiffness with the use of appropriate nanomaterials can direct MSCs to differentiate into specific lineages. Soft matrices ( $E \sim 0.1\text{--}1 \text{ kPa}$ ) that mimic brain are neurogenic, stiffer matrices ( $E \sim 8\text{--}17 \text{ kPa}$ ) that mimic muscle are myogenic, and comparatively rigid matrices ( $E \sim 25\text{--}40 \text{ kPa}$ ) that mimic collagenous bone are osteogenic [35]. Due to their favorable mechanical and electrical properties, GFs, *i.e.*, 3D derivatives of graphene, have proven compatible scaffolds for neural [36], muscle [37], and cartilage [38] tissue engineering. Compared to 2D graphene films, 3D-GF scaffolds can support the growth of neural stem cells (NSCs) *in vitro* and maintaining them in an active proliferation state via upregulation of Ki67 expression. 3D-GFs also enhanced NSC differentiation into astrocytes and neurons and proved to be an efficient conductive platform to mediate electrical stimulation of differentiated NSCs [36]. Other studies have demonstrated that 3D-GF bioscaffolds facilitate the growth and differentiation of C2C12 myoblasts into functional myotubes [37], and maintain the viability of ATDC5 chondrocyte progenitor cells [38]. Graphene foam-based hydrogel scaffolds were shown to be an attractive therapy for treatment of DPNI (diabetic peripheral nerve injury) due to their excellent mechanical strength, porous network, superior electrical conductivity, good biocompatibility, and ability to deliver adipose derived stem cells (ADSCs) [39]. *in vitro* results revealed that these scaffolds accelerated the proliferation of Schwann cells and *in vivo* experiments demonstrated that ADSC-loaded GF/hydrogel scaffolds promoted revascularization of target muscles and inhibited the atrophy of muscle fibers (Fig. 3). Functionalized

**Fig. 3** **A–F** Treatment of diabetic peripheral nerve injury using graphene foam scaffolds, with and without encapsulated ADSCs and their comparisons with ADSC-alone treatment for tissue regeneration potential by quantifying morphology changes and revascularization of targeted muscles (adapted with permission from [39]): **(A)** Images of gastrocnemius muscles, **(B)** quantitative analysis of the relative wet weight of gastrocnemius muscles, **(C)** Masson staining of muscles (scale bar = 50  $\mu\text{m}$ ), **(D)** quantitative analysis of the average diameter of fibers, **(E)** CD31 staining of gastrocnemius muscles (scale bar = 50  $\mu\text{m}$ ), and **(F)** quantitative analysis of microvessel density of gastrocnemius muscles. **G–I** Enhanced cardiac repair and cardiac function restoration by implantation of MSC-rGO hybrid spheroids (adapted with permission from [48]): **(G)** Capillary density in the periinfarct border zone assessed by immunostaining for vWF (green) (scale bar = 100  $\mu\text{m}$ ), **(H)** cardiac fibrosis indicated by Masson's trichrome staining (blue) and quantification of the fibrotic area, and **(I)** Expression of Cx43 (red) examined by immunohistochemical staining in the infarct border zone (scale bar = 100  $\mu\text{m}$ ). Infarcted hearts were treated through the injection of PBS, rGO flakes, MSC spheroids (Sph-0), or MSC-rGO hybrid spheroids (Sph-5)



graphene derivatives can also be used as an additive to synthetic polymers, such as polycaprolactone (PCL), poly(vinyl alcohol) (PVA), and poly(lactic-co-glycolic acid) (PLGA), as well as naturally occurring polymers such as chitosan, cellulose, hydroxyapatite, silk, collagen, and gelatin to improve their mechanical properties. When GO

was incorporated into PVA hydrogels, the resulting composite showed increased tensile and compression strengths without impacting biocompatibility [40]. A hierarchically porous hydroxyapatite hybrid scaffold containing rGO was found suitable for bone repair as it resulted in regenerated bone with enhanced volume (more than twice) and

mechanical properties (more than sevenfold) [41]. Another study established the superiority of graphene mesh supported double-network hydrogel scaffolds loaded with netrin 1 over autologous grafts for peripheral nerve regeneration. These hydrogels had an acceptable Young's Modulus of  $725 \pm 46.52$  kPa, matching with peripheral nerves, as well as a satisfactory electrical conductivity of  $6.8 \pm 0.85$  S/m and promoted the proliferation of Schwann cells and guided their alignment [42]. GO-alginate microgels with antioxidant activity, containing encapsulated mesenchymal stem cells (MSCs) and fabricated using electrospraying, were found to be an effective platform for repair of cardiac tissue post myocardial infarction [43]. The authors found that antioxidants co-encapsulated in graphene-alginate microgels improved stem cell survival and therapeutic efficacy, resulting in a significant decrease in infarction area, higher viability of cardiomyocytes and an improvement of cardiac function. Poly(citric acid-octanediol-polyethylene glycol) (PCE) is a citric acid based biodegradable polymer. To make its physicochemical properties and degradation behavior suitable for skeletal muscle tissue regeneration, nanocomposites of PCE and graphene (PCEG) were developed, where PCE provided the biomimetic elastomeric behavior and rGO contributed to mechanical strength and conductivity [44]. These composite scaffolds significantly enhanced muscle fiber and blood vessel formation *in vivo* in a rat model of skeletal muscle lesion, thus showing potential for myogenic differentiation. Integration of GO into PLGA also improved its surface (hydrophilicity) and mechanical (storage and loss moduli) properties, resulting in improved biocompatibility with neuronal cells [45].

A highly porous, hydrophilic, and mechanically strong aerogel of type I collagen, containing 0.1% GO, was found suitable for bone regeneration, where *in vitro* experiments exhibited better biomineralization rate and *in vivo* testing showed better bone repair effect in rat cranial defect models [46]. A decellularized bone scaffold decorated with magnesium nanoparticle enriched GO nanoscrolls (MgNPs@GNS) was shown to achieve vascularized bone regeneration in a rat cranial bone defect model. MgNPs@GNS induced an orchestrated inflammatory response, thus stimulating *in vitro* angiogenesis and osteogenesis through chemotactic, mitogenic and morphogenic actions [47]. By incorporating rGO flakes into MSC spheroids, their myocardial repair efficacy in infarcted hearts was improved (Fig. 3) [48]. Reduced GO shows high affinity towards ECM proteins, such as fibronectin, and has high electrical conductivity; these attributes resulted in enhanced cell-ECM interactions and enhanced expression of paracrine factors (angiogenic growth factors) and Cx43 (a gap junction protein) [48]. A photo-cross-linked gelatin hydrogel, reinforced with gelatin-rGO

(GOG), showed rapid bone repair capability of calvarial defects *in vivo* as it provided a porous microenvironment and the essential bioactive signals for bi-directional differentiation of bone marrow stromal cells (BMSCs), including angiogenesis and osteogenesis [49].

In a recent study, a hybrid dental implant consisting of graphene–chitosan (GC) nanocomposites coated onto titanium was found to promote osteoblast proliferation while reducing biofilm formation and bacterial activity [50]. 1% GO was found optimal for modulation of the implant's surface properties, such as wettability and surface roughness, to see this effect. Injectable gelatin methacrylate (GelMA) hydrogels were impregnated with polyethyleneimine-functionalized GO nanosheets (fGO) to achieve local delivery pro-angiogenic genes for myocardial infarction repair and vasculogenesis [51]. In this study, fGO nanosheets were functionalized with vascular endothelial growth factor (VEGF) DNA to achieve sustained local delivery of the pro-angiogenic gene. Characterizations *in vitro* and *in vivo* using rat models of myocardial infarction showed increased vascularity from GelMA containing fGO-DNA<sub>VEGF</sub> compared to both GelMA containing DNA<sub>VEGF</sub> and fGO each. These studies collectively indicate graphene (particularly GO) has the potential to be used as an additive in a variety of synthetic and natural polymers, providing essential chemical and physical cues, generating a suitable micro-environment, retaining and/or enhancing mechanical properties of the composite, and improving cellular response for effective regeneration of functional tissues. Detailed information about the regeneration of different tissues, according to the type of graphene derivatives used in the scaffold, is listed in Table 1.

## 2.2 Cell adhesion and differentiation

Graphene and its derivatives have been found valuable nanomaterials for stem cell research, due to their remarkable electro-conductivity, stiffness, and nanoscale topography [33]. These properties enable graphene to promote proliferation and differentiation of a variety of stem cells, including embryonic, mesenchymal, neural, and adipose stem cells as well as induced pluripotent stem cells (iPSCs), into different lineages for tissue engineering, regenerative medicine, and cell therapy applications [33, 52–55]. Graphene and GO coated glass surfaces were found useful platforms for iPSC culture, where surface properties dictated the degree of cell adhesion and proliferation rate as well as the type of lineage (*i.e.*, ectodermal, mesodermal, endodermal) that iPSCs differentiated into [52]. Graphene coated SiO<sub>2</sub>/Si substrates was shown to stimulate the adherence and growth of both human osteoblasts and mesenchymal stem cells (hMSCs) [53]. The

**Table 1** Tissue engineering scaffolds of graphene

Type	Modification	Characteristics	Applications	References
Graphene	PolyGelMA (gelatin methacrylate) loaded with netrin-1	Nickel mesh tube hydrogel scaffolds with enhanced mechanical property	Hydrogel conduit for peripheral nerve regeneration	[42]
	Graphene foam/hydrogel scaffolds	Metal bar dependent scaffold diameter	Peripheral regeneration in diabetic mouse model	[39]
GO	Injectable GelMA hydrogels, reinforced with GO	Enhanced modulus to inject hydrogel	Intramyocardial injection for regeneration of infarct rat heart	[51]
	Collagen composite aerogel	Enhanced stiffness and water retention	Rat cranial bone regeneration	[46]
	Magnesium nanoparticles (MgNPs) decoration	Scrolled structure	Rat cranial bone regeneration and vascularization	[47]
rGO	Incorporation with hydroxyapatite	Hierarchically porous scaffolds with enhanced porosity and degradability	Induced rat bone regeneration with HA/rGO-6/0.3	[41]
	MSCs encapsulation with alginate microgels	Changed color and $I_D/I_G$ ratios according to the reduction time	Regeneration of infarcted hearts through antioxidant activity	[43]
	Poly (citric acid-octanediol-polyethylene glycol)(PCE) nanocomposites	Enhanced mechanical properties and stability	Rat skeletal muscle injury repair	[44]
	MSC hybrid spheroid	Enhanced spheroid viability	Treatment of mouse infarct region	[48]
	Gelatin hydrogel	Winkled and curled fabric structure	Rapid rat bone regeneration	[49]

acceleration in differentiation of hMSCs into osteogenic lineage caused by graphene can be explained by its strong non-covalent binding capabilities (*i.e.*,  $\pi$ - $\pi$  stacking, hydrogen bonding, and electrostatic interactions) with growth factors and osteogenic inducers typically added to the medium [54] (Table 2).

Another study used composite scaffolds of poly(3,4-ethylenedioxythiophene) (PEDOT) and GO nanosheets to study differentiation of neural stem cells (NSCs) [56]. Carboxylic acid functional groups provided by GO were used to covalently crosslink with biomolecules to promote targeted differentiation. The surfaces modified with interferon- $\gamma$  (IFN- $\gamma$ ) supported a larger population of neurons and those modified with platelet-derived growth factor

**Table 2** Tissue engineering scaffolds of CNTs

Type	Modification	Characteristics	Applications	References
SWNTs	Dispersion of SWNTs in hyaluronic acid solution	Enhanced mechanical properties and hydrophilicity	Guided rat calvaria bone regeneration	[96]
	SWNT-reinforced electrospun chitosan-gelatin scaffolds	-COOH functionalized SWNTs, fiber length < 100 nm and diameter 1 nm	Cartilage tissue engineering	[97]
MWNTs	CNT coated bacterial cellulose scaffolds	CNTs modified with an amphiphilic comb-like polymer	Regeneration of bone defects in mouse model	[93]
	MWNT-reinforced electrospun PCL-collagen fibers	Length of 8–12 $\mu$ m and diameter of 10–12 nm, enhanced conductivity and mechanical properties	Directional regeneration of peripheral nerves	[95]
	Injectable composite scaffolds of CNTs and methacrylate-grafted elastin and gelatin	High conductivity and flexibility led to synchronous contractions, cardiac function restoration	Repair of heart muscle post myocardial infarction in rats and minipigs	[94]
	MWNT-reinforced PLA/PCL nanofiber mats	-COOH functionalized, fiber length 0.5–2 $\mu$ m and diameter < 8 nm	Fibrocartilage regeneration in rabbit temporomandibular joint disc defects	[98]
	CNT yarns inserted in silicon tubes	Tube length 300 $\mu$ m and diameter 10 nm, aligned fibrous structures inside the silicon tube	Axonal regeneration in peripheral nerve defect	[99]

(PDGF) supported a larger population of oligodendrocytes [56]. Not only molecular surface modifications, but nanoscale topography of the substrate can also heavily influence cell growth. For example, glass coated with GO films showed stronger affinity for hASCs and enhanced differentiation into specific cell types via osteogenesis, adipogenesis, and epithelial genesis [57]. Factors influencing graphene-induced differentiation can be summarized as follows: (a) biomolecule interaction, (b) cell membrane interaction, (c) surface topography and stiffness, and (d) electrical properties [58]. Biomolecules and cell membranes interact with graphene through electrostatic interactions,  $\pi$ - $\pi$  bonds, and hydrogen bonding, thus promoting intracellular cascades and modulating cell response via cell signaling pathway. Moreover, the nanoscale topographical cues of graphene improve cell anchorage and induce mechanosensitive pathways and cytoskeletal changes in the cells that promote differentiation.

### 2.3 Cytotoxicity

**Graphene:** The cytotoxicity of graphene is well investigated and its effects on a variety of cell types, ranging from macrophages and kidney cells to lung epithelial cells and fibroblasts, have been found dose-dependent [59–63]. Many studies indicate that the cytotoxicity of graphene is mainly influenced by its concentration, surface chemistry, and morphology. Appropriate surface modifications, *e.g.*, functionalization with carboxyl groups, can alleviate concerns of graphene cytotoxicity [60]. The adverse effects of graphene are attributed to the reactive oxygen species (ROS) formed when graphene is introduced to the system. Accumulation of graphene can cause significant rise in the levels of ROS in both intra- and extracellular environments, which further inhibits the nutrient uptake of cells. Graphene-induced ROS-activated apoptosis occurs through the MAPK and TGF- $\beta$  signaling pathways [59]. **Graphene Oxide:** GO causes dose-dependent oxidative stress; it is not blatantly toxic at low concentrations but induces ROS-mediated cell death at higher concentrations [61]. In human fibroblast cells, GO was not cytotoxic at  $< 20 \mu\text{g/mL}$  and had obvious cytotoxic effects, including cell apoptosis, at  $> 50 \mu\text{g/mL}$  [63]. In mice, low (0.1 mg) and middle (0.25 mg) doses were not cytotoxic, but high doses (0.4 mg) cannot be cleaned by the kidney and exhibit chronic toxicity, including lung granuloma formation [63]. Both graphene and SWNTs induce concentration- and shape-dependent cytotoxic effects [62]. Lactate dehydrogenase levels were found to be significantly higher for SWNTs compared to graphene. Moreover, ROS were generated in a concentration- and time-dependent manner after exposure to graphene (indicating an oxidative stress mechanism) and exposure to  $10 \mu\text{g/mL}$  graphene resulted

in caspase 3 activation (indicating apoptosis). Another study revealed that at equivalent dosage/concentration and equivalent surface chemistry, the cytotoxic effects of nanographite (or solvent-exfoliated graphene) on murine macrophages were higher than those induced by CNTs and carbon black [64]. **Reduced Graphene Oxide:** The cytotoxicity of rGO was shown to be triggered by reduction condition; the cytotoxicity of ferrous iron-reduced GO was lower than the cytotoxicity of light-reduced GO. Due to reduction-induced aggregation of ferrous iron, the cellular uptake was significantly declined [65]. Domínguez et al. compared the cytotoxicity of GO and rGO using human intestinal Caco-2 cell line and revealed that both GO and rGO caused cellular internalization and oxidative stress. Interestingly, cytotoxicity was only observed for rGO, not for GO at the concentrations tested [66]. Ezzati et al. developed amino acids-functionalized three-dimensional graphene foam and found its cytotoxicity to be time-dependent; alanine-anchored graphene foam had the lowest cytotoxicity [67]. Use of graphene in tissue engineering applications must take into careful consideration toxicological effects depending on its concentration, size, shape, surface chemistry and degree of oxidation (for example, lower oxidation degree causes higher oxidative damage to cells) [68]. If designed properly at the molecular level, graphene can advance the safety and efficacy of carbon-based nanomaterial scaffolds in biomedicine (Table 3).

### 2.4 Biodegradation

Besides toxicity, the rate at which graphene degrades *in vivo* is of paramount importance. Given the widespread presence of  $\text{H}_2\text{O}_2$ , a strong oxidizing agent, in the body and environment, the rate of degradation of graphene was found to depend on  $\text{H}_2\text{O}_2$  concentration [69]. In addition, holes or defect sites were first generated by random attack of  $\text{H}_2\text{O}_2$ , followed by a progressive destruction of carbon-carbon bonds of graphene around the initial defect sites. Kotchey et al. revealed that horseradish peroxidase (HRP), in the presence of low concentrations of  $\text{H}_2\text{O}_2$  ( $\sim 40 \mu\text{M}$ ), can cause the biodegradation of GO through enzymatic oxidation by inducing formation of holes on its basal plane [70]; the diameter of hole increases as time goes on. Unlike GO, HRP failed to degrade chemically reduced GO (RGO) because the heme active sites of GO have more affinity to HRP than those of rGO.

## 3 Carbon nanotubes

Carbon nanotubes are formed when carbon atoms, held together by  $\text{sp}^2$  bonds in a 2D structure, alternatively labeled graphene, are rolled up to form a 3D tubular



**Table 3** Tissue engineering scaffolds of nanocellulose

Type	Modification	Characteristics	Applications	References
CNCs	Reinforcing filler in PCL/chitosan scaffold	Strength ( $\sim 40$ MPa) and stiffness ( $\sim 500$ – $600$ MPa) of scaffold matched the properties of target tissue	Tendon and ligament tissue engineering	[138]
	Reinforcing filler in PLA scaffold	Enhanced mechanical properties and superior osteogenic potential	Bone regeneration	[145]
	3D printed and crosslinked alginate/gelatin/CNC scaffold	Enhanced mineralization efficiency of scaffold containing 1% CNC	Rapid bone regeneration in a rat calvaria critical-sized defects (CCD-1) model	[151]
	Reinforcing agent in chitosan, alginate, and hydroxyapatite scaffold	Enhanced porosity, swelling ratio and compressive strength	Bone tissue engineering	[152]
CNFs	Regenerated CNFs and poly(globalide) films formed via layer-by-layer assembly	Supported keratinocyte attachment and proliferation	Skin regeneration	[144]
	Carboxylated and phosphonated CNFs as reinforcing fillers in gelatin scaffold	Higher mineralization potential	Bone regeneration	[148]
	Gelatin, reinforced with TEMPO-CNF and HA nanoparticles, and crosslinked by glutaraldehyde	Enhanced Calvarial osteoblast cell proliferation and differentiation	Bone tissue engineering	[149]
	Chitosan and CNF composite hydrogels	Suitable rheological properties for disc restoration	Intervertebral disc tissue regeneration in pig and rabbit spine models	[150]
	CNF reinforced gelatin/chitosan composites	Tunable compression modulus (ranging between 10 kPa and 1 MPa), favorable for soft tissue regeneration	Cartilage tissue engineering	[154]

structure (Fig. 4). This simple 3D structure lends CNTs unique properties, such as exceptional mechanical strength (Young's modulus ranging between 0.27 and 1.34 TPa, tensile strength ranging between 11 and 200 GPa), as well as electrical and thermal conductivity ( $10^4$  S/cm<sup>2</sup> and 5000 Wm<sup>-1</sup> K, respectively); in addition, their tailorable physical and chemical properties make them useful additives in polymer composites [71] and a valuable platform for use within the biological system (Fig. 4) [72–75]. When these cylindrical nanostructures are composed of a single layer of graphene, they represent single-walled carbon nanotubes (SWNTs) whose diameter ranges between 1 and 2 nm, and when multiple layers of graphene are rolled about the lumen, they make up multi-walled carbon nanotubes (MWNTs) whose diameter ranges between 10 and 100 nm [5].

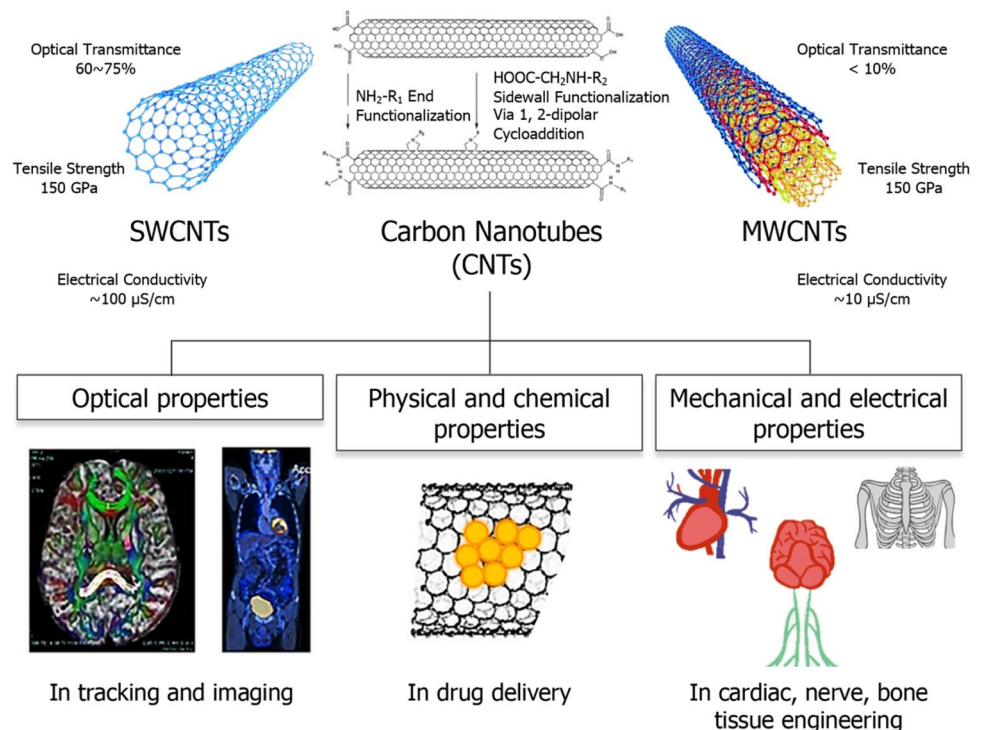
CNTs' tunable surface properties (via covalent or non-covalent functionalization) and high aspect ratio ( $> 1000$ , as lengths typically range between 50 nm and 1 cm), are highly desirable for enhanced interaction with biomolecules and cells per unit surface area. Their favorable physical dimensions and modifiable surface chemistry are attributes that allow adsorption of a wide variety of therapeutic biological molecules for drug/gene delivery and cancer therapy [76]. In the biomedical field, functionalized SWNTs are valuable tools for biosensing [77] and

bioimaging, for example, photoacoustic and photothermal detection of circulating tumor cells [78–81]. MWNTs, on the other hand, are typically preferred as additives in polymeric scaffold materials for tissue engineering applications due to their higher mechanical strength [19, 82, 83]. Chemical functionalization can alter the physical and biological properties of CNTs. While non-covalent modifications better preserve the *sp*<sup>2</sup> bonding structure of CNTs and their electronic characteristics, other modifications can be used to make the structure more biocompatible; for example, coating SWNTs with dextran sulfate to avoid opsonization and phagocytosis [84–86]. Biological tissues are transparent to NIR radiation, making the NIR photoluminescence property of CNTs useful for minimally invasive or non-invasive therapeutic and diagnostic applications, collectively termed theranostics [87–91]. Here, we discuss how CNTs are being used to advance the field of tissue engineering by offering possibilities for fabrication of robust polymeric scaffolds that increase cell adhesion, growth, and differentiation.

### 3.1 Tissue scaffolds

Composite scaffolds are meant to host many different cell types, while allowing for the natural biochemical flux to occur unhindered, such that nascent cells can grow and

**Fig. 4** Schematic illustrating carbon nanotubes (CNTs), both single-walled CNTs (SWCNTs) and multi-walled CNTs (MWNTs), and their unique optical, mechanical, and electrical properties, that make them versatile materials for diverse biomedical applications, including, but not limited to, medical imaging, drug delivery, and tissue engineering (partly adapted with permissions from [72, 81, 175])

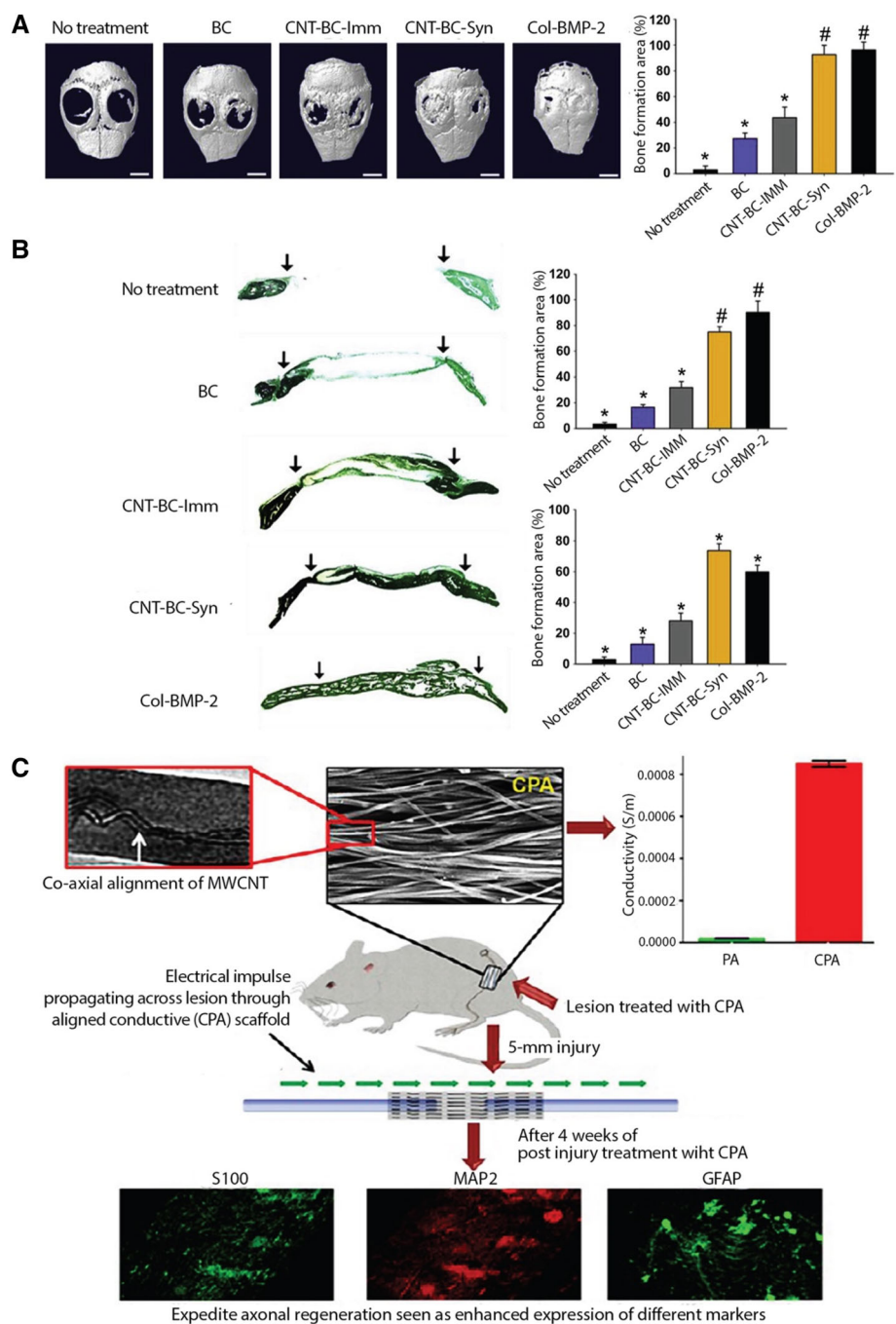


differentiate into mature tissue that mimics the native organ tissue. It is important that engineered scaffolds maintain at least the level of stiffness and mechanical strength that the native tissues have. If these minimum strength requirements are not met, then catastrophic breakdown of the scaffold *in vivo* can occur, resulting in the failure of regeneration. This is especially true in areas such as bone and cardiac tissues, where mechanical and tensile strength is paramount to the success of the scaffold. While bone scaffolds need to be able to match the stiffness of surrounding tissues, cardiac scaffolds must also survive the constant cyclic contractions of the adjacent tissue and the developing tissue that it is supporting. Synthetic polymers, such as PCL, PVA, and PLGA, as well as natural polymers like chitosan, gelatin, hyaluronic acid, etc., have been shown to be promising scaffold materials; however, their mechanical properties are inferior. Recent research has shown that the addition of CNTs to polymeric scaffolds results in drastic improvement of their mechanical properties [19, 83]. However, CNTs are vastly underutilized for tissue scaffolds and there is much room to realize their full potential.

Conductive CNT/silk fibroin scaffolds, fabricated via electrospinning, were found compatible with neonatal rat cardiomyocytes, and enhanced the expression of cardiac specific proteins and the formation of sarcomeres and gap junctions. Control of nanofiber alignment in the scaffolds guided the oriented organization of cardiomyocytes, thus biomimicking the native myocardium and showing

potential for effective regeneration of functional cardiac tissue [92]. *In vivo* testing in a mouse model showed that the use of 3D composite scaffolds of bacterial cellulose (BC) and CNTs, especially those containing modified CNTs, showed excellent bone regeneration efficacy (Fig. 5) [93]. Due to their high electrical conductivity, CNTs have shown promise in cardiac regeneration too. For example, injectable patches, consisting of methacrylated elastin, gelatin and CNTs, with a hierarchical porous structure and shape-memory behavior, were fabricated for the repair of infarcted cardiac muscle in rat and porcine models [94]. Interestingly, the flexible and conductive scaffolds containing a high concentration of CNs (55% w/w), provided a favorable microenvironment for the functional repair of ligated left anterior descending coronary artery in rats after 4 weeks, fractional shortening and ejection fraction were increased, infarcted area was decreased, and functional recovery of infarcted hearts in minipigs was observed as indicated by improved revascularization. In another study, CNTs were used to achieve guided peripheral nerve regeneration, without compromising the biodegradability and biocompatibility of the scaffold. Co-axially aligned electrospun scaffolds of PCL and collagen, containing MWNTs, were found efficient in healing injured sciatic nerves in rats within 30 days [95]. The anisotropic electrical conductivity of MWNT-reinforced fibrous scaffolds was 85% higher along the direction of alignment, resulting in improved axonal regeneration *in vivo* (Fig. 5).

**Fig. 5 A–B** Bone regeneration efficacy of CNT-BC composite scaffolds evaluated in mouse calvarial defects for 8 weeks (adapted with permission from [93]). Collagen scaffolds loaded with bone morphogenetic protein-2 (BMP-2) (Col-BMP-2), a clinically used bone graft, served as a positive control. Amphiphilic comb-like polymer (APCLP) was used to modify/coat CNTs: **(A)** Bone regeneration evaluated by micro-CT analyses and quantification of the bone formation area in defects and **(B)** Goldner’s trichrome staining of mouse calvarial defect areas and quantification of bone formation area and new bone density in defects. CNT-BC-Syn represents APCLP-coated CNT-BC hybridization and CNT-BC-Imm represents scaffolds prepared by immersing BC in APCLP-coated CNT solution. Arrows indicate the bone defect margin. **C** MWCNT-reinforced, aligned PCL-collagen (CPA) scaffolds for directional peripheral nerve regeneration (adapted with permission from [95]). Higher anisotropic conductivity of CPA scaffolds led to more efficient healing of injured sciatic nerves in rats, as indicated by immunohistostaining of S100, MAP2, and GFAP proteins, 30 days after implantation



A CNT-based membrane, formed by dispersing SWNTs in hyaluronic acid, was used to cover experimental bone defects made in rat calvaria [96]. 8 weeks after surgery, more extensive bone formation occurred in membrane covered defects compared with bone defects not covered by a membrane. The adequate strength and surface characteristics of the CNT-based composite resulted in cellular shielding properties (preventing entry of non-osteogenic cells such as epithelial cells and fibroblasts) and inducing osteogenesis (promoting proliferation of osteoblasts) [96]. Electrospun nanocomposite scaffolds of chitosan and gelatin, containing 1% of COOH-

functionalized SWNTs, were found to be biocompatible and have suitable physicochemical properties for cartilage tissue engineering applications [97]. Temporomandibular joint disc (TMJD) has a complex microstructure and poor regenerative capacity. Biomimetic properties of electrospun scaffolds of PCL/PLA/COOH-functionalized MWNTs, attributed to their regionally anisotropic microstructure and biconcave anatomy, were found to result in guided TMJD regeneration and subchondral bone protection [98]. The biocompatibility and repair properties of these composite scaffolds were verified *in vivo* in nude mice as well as rabbits. MWNT-based

scaffolds have been found effective for peripheral nerve regeneration, where 2% CNT density was the most effective in repairing 15 mm sciatic nerve defects in rats, as measured by both histological axonal regeneration and motor function [99]. Because CNTs can improve the electrical conductivity and mechanical properties of polymers, CNT-reinforced composites have typically found more utility in cardiac, nerve and bone tissue regeneration.

### 3.2 Cell adhesion and differentiation

A nanostructured CNT–chitosan hybrid layer provided a biocompatible biointerface on metallic (*i.e.*, Ti) implants, lending them topological features useful for bone regeneration [100]. These hybrid composites were observed to stimulate osteoblastic cell adhesion and growth via increased expression of adhesive proteins and have significantly enhanced protein adsorption rates due to electrostatic interactions between the positively charged CNT–chitosan surface and negatively charged proteins. CNT-coated PCL nanofiber scaffolds were found to have surface properties favorable for tissue healing and bone regeneration as these were highly effective in reducing inflammation, promoting angiogenesis, and driving adhesion and osteogenesis of MSCs *in vitro* [101]. A recent study demonstrated the impact of unzipping or oxidizing MWNTs using strong acid treatment on their biocompatibility and osteogenic potential. Compared to pure CNTs, unzipped CNTs (u-CNTs) exhibited better viability of bone marrow-derived MSCs because the presence of different functional groups (*e.g.*, hydroxyl and carboxyl groups) on their surface generated lower amounts of ROS in cell culture media [102]. The upregulation of osteogenic-associated gene markers in the case of u-CNTs confirmed their superior mineralization and bone regeneration potential.

Another study evaluated different types of functionalized carbon nanotubes (*i.e.*, COOH-SWNTs, COOH-MWNTs, and PEG-SWNTs) for their impact on the rate of proliferation of canine MSCs and the propensity of MSCs to differentiate into osteogenic, chondrogenic, and neurogenic lineages [103]. Detailed analyses showed that MSCs spread out better on all CNT films than on the control, but their rate of proliferation on all CNT films was slightly lower than those on the control. More importantly, while chondrogenesis was promoted by COOH-SWNTs, neuronal differentiation was promoted by both SWNTs and MWNTs. Overall, the less toxic environment (fewer apoptotic and necrotic cells) provided by COOH-functionalized CNTs, as well as their selective differentiation potential, indicated their promise for use as scaffold components in stem-cell based regenerative medicine. When the underlying processes, by which CNTs lead to cell attachment and spreading, were evaluated using different

cell types, including fibroblasts and neural-like cells, the mechanism was found to be the same for SWNTs and MWNTs [104]. Cell attachment and spreading onto individual SWNTs and MWNTs were integrin-dependent and facilitated by the adsorption of serum and cell-secreted adhesive ECM proteins to the nanotubes. With our increasing understanding of how cells interact with scaffold surfaces, conjoined with ever-increasing studies on chemical functionalization of CNTs for successful incorporation into polymeric scaffolds, the true impact of these nanostructures in the field of tissue engineering is beginning to look very promising. CNT's inherent electrical conductivity, which is especially important for regeneration of muscle and nerve tissues, and other physicochemical properties, which can be tuned by suitable surface modifications, enable CNTs to support cell growth and differentiation through increased intercellular signaling.

### 3.3 Cytotoxicity

It is imperative that short- and long-term toxicity of CNTs is considered before their introduction into tissue scaffolds for *in vivo* use. Fortunately, the toxicity of CNTs is quite well-studied. The needle shaped structure of CNTs can cause damage to cell membranes and mitochondria via oxidative stress; high concentrations of CNTs have been shown to cause increased ROS production and reduced glutathione (GSH) levels [105]. In Nrf2 (nuclear factor erythroid 2-related factor 2) knockout mice, exposure to MWNTs by pharyngeal aspiration elicited rapid inflammatory and fibrotic responses in a dose and time dependent manner, with peak responses recorded on day 7 post-exposure to 40  $\mu\text{g}$  MWNTs [106]. This study revealed that Nrf2 plays an important role in suppressing the basal and MWNT-induced oxidant production, inflammation, and fibrosis in the lungs, thereby protecting against lung toxicity caused by MWNTs. Studies focused on SWNTs have shown dose-dependent cytotoxicity of CNTs on a range of cell types, including lung epithelial cells, keratinocytes, macrophages, cardiac cells, and hMSCs [107–111]. Studies focused on MWNTs have shown a similar phenomenon in epithelial cells, lung tumor cells, keratinocytes, and murine embryonic stem cells [112–116]. Depending on their surface area, dimensions, functionalization, dispersion and/or mode of introduction, the effects of MWNTs have been observed to range from non-cytotoxic to mildly cytotoxic [117]. A study investigated the toxicity of SWNTs and MWNTs *in vitro* (MC4L2 cells) and *in vivo* (mice) and found SWNTs to be more toxic, particularly at high dosages [118]. On the other hand, MWNTs, even at low dosages, had better therapeutic efficacy against breast cancer cells as compared to both SWNTs and Doxorubicin (a model anti-cancer drug).

Also, affecting their degree of cytotoxicity is the propensity of CNTs to aggregate due to strong electrostatic interactions. It was shown that CNT aggregate concentrations greater than or equal to 2.5  $\mu\text{g/mL}$  induced cellular death in murine macrophage cells [119]. However, these adverse cytotoxic effects can be mitigated by carefully choosing surface modifications that not only improve the biocompatibility of CNTs but also enable homogeneous and uniform dispersion in polymeric matrices. The aggregation impediment can be reversed by means of chemical, mechanical, or heat treatments. For example, COOH-functionalized SWNTs and those obtained by a combination of ultrasonication and acid treatment, were biocompatible with hMSCs and led to osteogenic and/or adipogenic differentiation [120, 121]. When comparing several different types of covalently modified MWNTs, induced pulmonary fibrosis in animal cells was found to be lower for CNTs functionalized with –COOH groups [122]. These data support the hypothesis that surface charge plays a crucial role in CNT-induced tissue damage. Finally, after multiple studies aimed at unraveling the cytotoxicity of both CNTs and graphene simultaneously, it has been determined congruently that graphene, regardless of its modification, presents a more toxic effect than CNTs. One such study was conducted on murine peritoneal macrophages. These data show that graphene and graphene derivatives are more potent in inducing cell death via autophagosome accumulation and lysosome impairment of macrophages, when compared to SWNTs at similar concentrations [123]. The cytotoxicity of CNTs in tissue engineering can be managed by modulating their physicochemical properties, including surface chemistry and size/aspect ratio, and dosages.

### 3.4 Biodegradation

Modugno et al. studied the enzymatic biodegradability of double- and multi-walled CNTs, of varying lengths, degrees of oxidation and different functionalizations, using HRP [124]. While all double-walled CNTs tested resisted biodegradation; some MWNTs were partially degraded, particularly those functionalized with amidation were found to have significantly shorter length and a high number of defects at the end of the treatment. Dispersibility also affected biodegradation as low dispersibility resulted in less interaction with HRP enzyme.

## 4 Nanocellulose

Cellulose accounts for approximately  $1.5 \times 10^{12}$  tons of natural biomass production each year and is the most abundant biopolymer on earth [125]. Cellulose is the

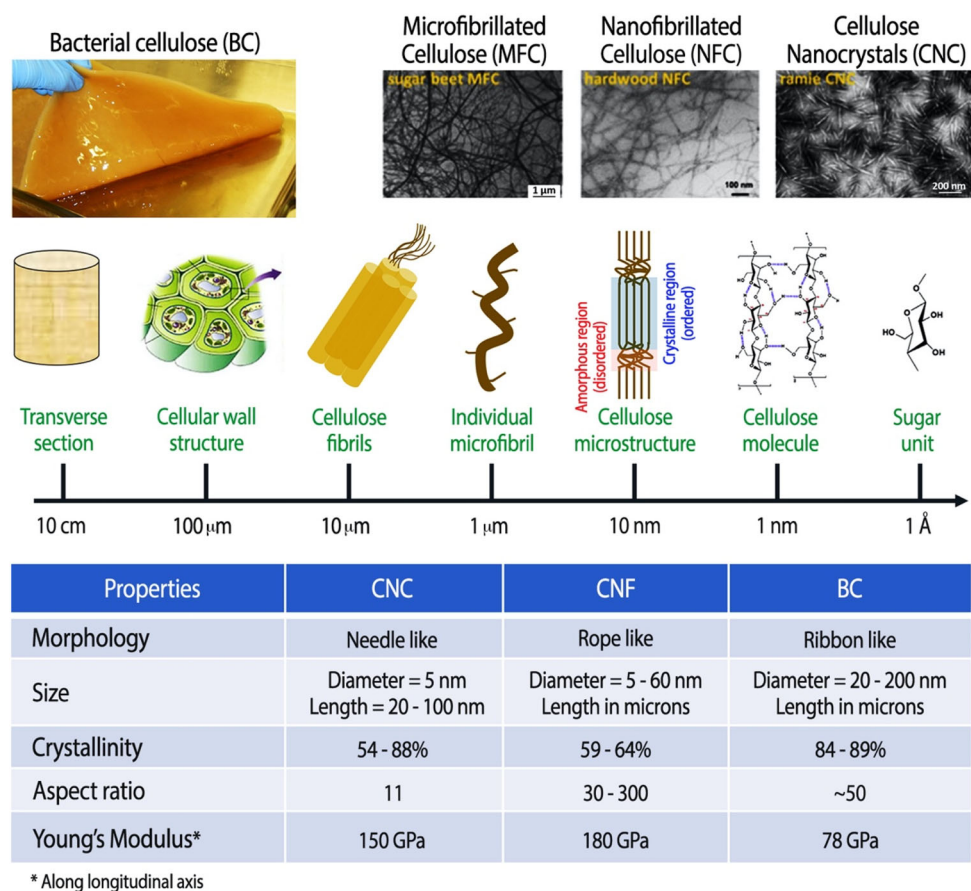
principal structural polysaccharide in plants and the main component of natural fibers (e.g., cotton) as well as man-made fibers (i.e., viscose) used in textiles. Its hierarchical structure consists of individual microfibrils (1  $\mu\text{m}$  diameter) that can be broken down into elementary nanoscale fibrillar and crystalline structures (Fig. 6) [126], whose dimensions depend on the source of cellulose and extraction conditions [125–129]. Rod- or needle-shaped cellulose nanocrystals (CNCs), with lengths ranging between 50 and 200 nm and widths ranging between 5 and 20 nm, and cellulose nanofibers (CNFs), with widths ranging between 5 and 50 nm and lengths up to several microns, are attractive materials for tissue engineering due to their unique physicochemical properties such as high aspect ratio, large surface area, reactive surface containing hydroxyl groups and modifiable surface chemistry [11, 130–132]. The extraordinary stiffness and strength (i.e., 110–220 GPa axial elastic modulus (E) and 7.5–7.7 GPa tensile strength ( $\sigma$ )) of CNCs are attributes that make them comparable to other reinforcement nanomaterials such as clay nanoparticles and carbon nanotubes [133]. Moreover, their biocompatibility, biodegradability, and low or no cytotoxicity make them very well suited for a variety of biomedical applications, including tissue engineering, targeted drug delivery, and bioimaging [130, 131, 134].

Bacterial cellulose (BC) is a highly crystalline form of nanocellulose, synthesized by bacteria, with excellent wettability, stiffness, and tensile strength; a comparison of its properties with those of CNCs and CNFs is provided in Fig. 6 [135]. The porous, fibrillar web-like structure of BC lends it ECM mimicking properties and makes it a suitable material for scaffolds that promote cell adhesion and growth [10]. A few previous review articles have already discussed in detail the production and use of BC (pristine as well chemically modified *in situ* or *ex situ*) in tissue engineering, for example, vascular grafts, wound dressings, and bone regeneration scaffolds [10, 136, 137]. In the following sections, we highlight how the properties of nanocellulose, whether it is derived from plant-based sources, such as wood, cotton, etc., or bacteria, are promising for tissue engineering, particularly for regeneration of structurally oriented tissues such as skeletal muscle, tendons, ligaments, and nerves.

### 4.1 Tissue scaffolds

Cellulose nanocrystals have typically been used as reinforcing fillers to improve the mechanical strength of scaffolds made from synthetic polymers such as polycaprolactone (PCL), polylactic acid (PLA), polyvinyl alcohol (PVA), poly(ethylene oxide) (PEO), poly(ethylene glycol) (PEG), PLGA, as well as natural polymers such as

**Fig. 6** Top Hierarchical structure of cellulose, showing how macro-sized cellulose fibrils are made up of bundles of micron-sized individual microfibrils, and each microfibril can further be broken down into nanoscale fibrils and crystals (adapted with permission from [130]). Bottom A table comparing the structural properties of CNCs, CNFs, and bacterial cellulose [135]



chitosan, gelatin, alginate, hydroxyapatite and hyaluronic acid. These biocompatible polymers are suitable for tissue engineering applications, but they often lack the mechanical properties required to match those of native tissues that serve as target implantation sites, especially in the case of tissues such as skeletal muscle, tendons, and ligaments with load bearing functions. Three-dimensional scaffold structures containing cellulose nanocrystals or nanofibers can be prepared using a variety of techniques; however, electrospinning, a simple and scalable technique, is extensively used for fabrication of nanocellulose-based tissue engineering scaffolds because it is possible to process a variety of polymers with tunable fiber diameter and unique topographies using this method [138–141]. Incorporation of small amounts of CNCs (up to 3%) as reinforcing fillers into tendon-mimetic PCL-chitosan nanofibers demonstrated remarkable improvement in their mechanical properties (*i.e.*, tensile strength and stiffness) such that the composite scaffolds matched the properties of tendons and ligaments ( $\sigma$ ,  $\sim 40$  MPa and  $E$ ,  $\sim 500$ – $600$  MPa) (Fig. 7) [138]. The inherent property of cellulose nanocrystals to align in the scaffold matrix, particularly at high concentrations, helps induce alignment of target cells, making CNCs favorable reinforcing fillers

for tendon and nerve regeneration. This was demonstrated in a study where electrospun composite scaffolds, consisting of uniaxially aligned CNFs and CNCs embedded in the matrix, showed considerable orientation of CNCs along the long axis, making them useful for regenerating tissues such as blood vessels, tendons, and nerves where cell orientation is crucial. By incorporating 20% (w/w) CNCs, the tensile strength and elastic modulus of the scaffolds showed substantial enhancement along the fiber alignment direction, by 102 and 172%, respectively [142]. Moreover, the scaffolds were non-cytotoxic to human fibroblasts and the aligned composites exhibited a strong effect on directing cellular organization of human dental follicle cells (hDFCs).

Incorporation of 7% w/w CNCs in PLGA, an FDA-approved biocompatible and biodegradable polymer, was found optimum to fabricate nanofiber membranes with mechanical properties matching those of human skin, indicating the potential of PLGA/CNC composites for skin regeneration [143]. Another study synthesized bilayer films of regenerated CNFs and poly(globalide) via layer-by-layer deposition and found it to be a suitable scaffold for skin tissue engineering [144]. Produced from renewable plant-based materials, PLA is the most widely used

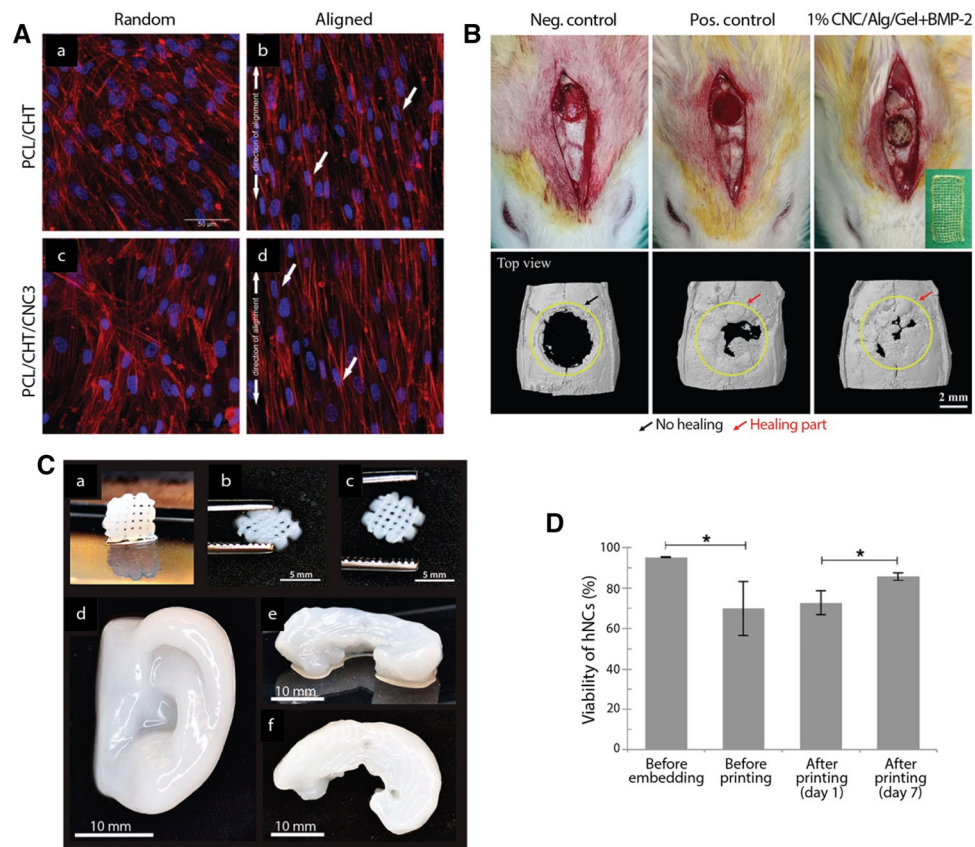


**Fig. 7** **A** Utility of anisotropically aligned, CNC-reinforced, PCL-chitosan-CNC scaffolds for tendon tissue engineering (adapted with permission from [138]). Confocal microscopy images of hTDCs seeded on PCL/CHT and PCL/CHT/CNC3 scaffolds with random and aligned topography, respectively. Organization of cytoskeletal actin filaments after 10 days of culturing hTDCs (blue: nuclei stained with DAPI; red: actin filaments stained with rhodamine-conjugated phalloidin). **B** 3D printed CNC-reinforced alginate-gelatin hydrogel scaffolds for bone tissue engineering (adapted with permission from [151]): (top) Digital photograph of *in vivo* surgical experiments and

(bottom)  $\mu$ CT images showing the extent of bone regeneration in rat calvaria defect model 3 weeks after transplantation. **C** 3D printed nanocellulose-alginate scaffolds for cartilage tissue engineering (adapted with permission from [158]): (a) 3D printed small grids ( $7.2 \times 7.2 \text{ mm}^2$ ) after cross-linking, (b) the shape of the grid deforms while squeezing, and (c) its restoration after squeezing. 3D printed human ear (d) and sheep meniscus side view (e) and top view (f). **D** Viability of human nasoseptal chondrocytes (hNCs) before and after 3D bioprinting (adapted with permission from [158])

biodegradable and biocompatible polymer to fabricate porous 3D structures that closely mimic ECM via electrospinning and 3D printing. However, PLA scaffolds suffer from poor mechanical properties and low hydrophilicity. Various studies have found CNCs to be excellent nanofillers in PLA for bone tissue engineering applications as they lead to enhanced mechanical and thermal properties, tunable biodegradation rate, and improved biocompatibility of the composite scaffolds [145–147]. For example, PLA/CNC composites had superior osteogenic potential than neat PLA, indicated by enhanced viability of seeded human bone-marrow-derived mesenchymal stem cells (BMSCs), higher expression of osteogenic gene markers in the attached cells, and higher mineralization on the surface of the scaffold [145]. This is one of the few studies that tested the scaffold *in vivo* and found the composite to have a higher bone regeneration

potential than the control, based on evaluation at the 3-week mark after transplantation in 2-month-old male rats. Another study used carbodiimide-based crosslinking to enrich gelatin scaffolds with two types of CNFs, *i.e.*, carboxylated and phosphonated CNFs. The mineralization and bone regeneration potential of composites containing 50% v/v functionalized CNFs was found to be higher, evident from the higher and more uniform deposition of calcium and hydroxyapatite type structures throughout the matrix and enhanced growth of MSCs [148]. Mechanically strong composite hydrogels of gelatin, TEMPO-oxidized (negatively charged) BC nanofibers and hydroxyapatite nanoparticles, crosslinked using glutaraldehyde, were found suitable for calvarial osteoblast proliferation and differentiation [149]. Non-cellularized injectable formulations of chitosan (1.7–3.3% w/w) and CNFs (0.02–0.6% w/w) were used as a minimally invasive approach to

regenerate damaged intervertebral discs [150]. The formulations became hydrogels *in situ* after intradiscal gelation and found to restore disc height and loss of mechanical properties in pig and rabbit spine models.

3D printed alginate-gelatin hydrogel scaffolds, reinforced with 1% CNCs, were found to result in a significantly enhanced expression of osteogenic-specific gene markers compared to control scaffolds without CNCs [151]. Moreover, *in vivo* testing revealed rapid bone regeneration in a rat calvaria critical-sized defects (CCD-1) model in the presence of the composite scaffold 3 weeks after transplantation (Fig. 7). Another study investigating the suitability of a composite of natural polymers, *i.e.*, alginate, chitosan, and hydroxyapatite, for bone tissue engineering found reinforcement with 1% CNCs to result in better attachment and proliferation of MG63 osteoblasts [152]. Composite scaffolds of polyhydroxybutyrate (PHB), a bioderived and biodegradable polymer, and CNF are superior candidates for bone tissue engineering than neat PHB due to their improved physicochemical properties (for example, crystallinity, water contact angle, degradation rate, biomineralization, mechanical toughness) and better human osteoblast MG63 cell viability [153]. CNCs and CNFs can be used to fabricate composites for regeneration of soft tissues too [154–157]. For example, adding 2% acetylated CNFs to PCL/gelatin electrospun scaffolds enhanced their hydrophilicity, degradation rate, tensile strength (comparable with those of skin tissue) and biocompatibility with L929 fibroblast cells [157]. Chitosan/gelatin composites, reinforced with CNFs, were found suitable for cartilage regeneration due to their hierarchical porous structure, suitable mechanical properties (compression modulus of about 1 MPa in dry conditions at room temperature, comparable with that of natural cartilaginous tissue, and lowered modulus of 18–32 kPa in PBS at 37 °C, favorable for soft tissue regeneration) and good compatibility with chondrocytes [154]. Another study was able to produce stable biocompatible 3D-printed nanocellulose-alginate scaffolds suitable for cartilage tissue engineering [158]; live human nasoseptal chondrocytes (hNCs) encapsulated in these scaffolds showed up to 85% viability 7 days after culture (Fig. 7). While these examples highlight the huge promise of CNC/CNF based composite scaffolds for engineering a variety of tissue types, there is still limited *in vivo* research.

## 4.2 Cell adhesion and differentiation

Nanocellulose, on its own, lacks the chemical cues to interact with biomolecules and cells. Nanocellulose based composites, however, have also shown promise for promotion of cell adhesion, growth, and targeted differentiation, with appropriate modification of the surface with

chemical groups and biological molecules. Hybrid fibers of cellulose acetate (CA) and PCL, blended in different ratios, were given post-electrospinning treatment with NaOH (also called alkaline saponification) which transformed CA into cellulose (CL), an otherwise barely spinnable polymer [140]. Not only did this treatment improve mechanical properties (Young's Modulus by ~ 20–30-fold, tensile strength by ~ 3–4-fold, and tensile stress by ~ 2–4-fold) of the composite, the presence of functional groups (OH) on its highly wettable surface enhanced its ability to nucleate bioactive calcium phosphate crystals throughout the matrix when exposed to simulated body fluid. The nanofibrous composite membranes also supported MC3T3-E1 cell (osteoblasts) proliferation [140]. Highly porous composite scaffolds of poly-(butylene succinate) and CNCs have successfully been fabricated with improved *in vitro* degradation rate and excellent biocompatibility with 3T3 fibroblasts [141, 159]. Injectable hyaluronic acid (HA)-based hydrogels are a class of promising materials for tissue engineering and regenerative medicine applications. A recent study fabricated a novel composite of chemically modified HA, reinforced with aldehyde modified CNCs; composite hydrogels were stiffer, had higher resistance to degradation and exhibited pronounced proliferative activity of human adipose derived stem cells (hASCs) [160].

Electrospun nanocomposite scaffolds fabricated using maleic anhydride grafted PLA, reinforced with CNCs, were found to support the proliferation of human adipose-derived stem cells (hASCs) [146]. Another study used 5% CNCs, grafted with PEG, to enhance the tensile strength of PLA scaffolds and improve their biocompatibility with human BMSCs [147]. Surface modification of nanocellulose composites with specific peptides and growth factors to make them more biomimetic has been tested in several studies [161–163]. For example, incorporation of osteogenic growth peptides (OGPs) in nanocomposite scaffolds, composed of BC, collagen, and apatite, were shown to induce early development of osteoblastic phenotype [161]. These composites did not show any cytogenic, mutagenic, or cytotoxic effects, and composites containing BC facilitated better cell growth, indicating the importance of this component in the scaffold's tissue regeneration potential. In another study, fibroblast-derived adhesion proteins, such as collagen and fibronectin, were immobilized on BC to modify its surface and mimic soft ECM chemistry [162]. Most importantly, they activated integrin adhesion pathways that generate stronger cell adhesions. Also, higher levels of mitochondrial activity and cell growth were observed on modified-BC scaffolds compared to non-modified controls. Biomimetic BC scaffolds, coated with soluble collagen I, were found potent in stimulating further collagen I production by MSCs seeded onto their surface, leading to the formation of a highly ordered, long-lasting



collagen network at the cell-material interface that supported multilayered growth and tight adherence of cells to BC surface [163]. Moreover, these scaffolds stimulated MSCs towards osteogenic differentiation.

### 4.3 Cytotoxicity

The cytotoxicity of CNCs and CNFs is very well studied and summarized in a recent review article [164]; the main takeaways are that (a) both CNCs and CNFs have a dose-dependent effect on cells and (b) CNCs show higher cytotoxicity than CNFs. Here we highlight a few studies that have looked at the *in vitro* and *in vivo* cytotoxicity of nanocellulose. A densified BC implant (containing 17% cellulose), suitable for auricular cartilage reconstruction due to similarity in mechanical strength, showed no cytotoxicity against L292 fibroblasts [165]. Another study evaluated the safety and efficacy of a BC wound dressing and no cytotoxic effects on L292 mouse fibroblast cells were observed; in fact, it promoted cell migration as good as the commercially available dressing material [166]. A study confirmed the impact of particle length on the cytotoxicity of CNCs and CNFs using two cell types, *i.e.*, macrophages and hepatocytes [167]. Interestingly, all CNC groups caused cytotoxicity in Kupffer cells, and one CNC group triggered cytotoxicity in hepatocytes. It was found that CNCs induce mitochondrial ROS generation, apoptotic cell death, lysosomal damage, and inflammation. On the other hand, CNFs did not induce cytotoxicity to cells because of the minimal cellular uptake. Another study looked at the fate of individual CNC particles in different cells. Cellular uptake of wood-derived CNCs by primary human brain microvascular endothelial cells and flax-derived CNCs in human HEK 293 and insect sf9 cell lines was confirmed using fluorescent probes [168]. The mechanism of CNC interaction with the cell membrane majorly depended on its surface charge and the type of functional groups on the surface. For example, fluorescein-labeled CNCs (negatively charged) were not taken up by the cells and caused cell death via plasma membrane rupturing, whereas rhodamine-labeled CNCs (positively charged) underwent endocytosis and displayed no evidence of cytotoxicity. A recent study assessed the toxicity profile of wood-derived CNFs and found that a concentration of 50 µg/mL did not affect the cytotoxicity or metabolic activity of fibroblasts and keratinocytes [169]. In an aerogel form, CNFs induced a reduction in the metabolic activity of these cell types but no significant cell death.

*In vivo* biocompatibility testing of BC wound healing membranes, implanted subcutaneously in a rat, showed no macroscopic evidence of inflammation such as redness and edema or exudates around the implanted region 3, 14 and 56 days after implantation [170]. However, oxidized BC

seemed to attract fewer inflammatory cells (neutrophils, macrophages, lymphocytes and polymorphonuclear cells) than the pristine material, which is generally considered highly biocompatible, and on the other hand gave rise to a thicker fibrosis compared to non-oxidized BC. Overall, BC membranes were found well integrated with the rat connective tissue, thus confirming minimal foreign body reaction. Another study found the *in vivo* biocompatibility index of a densified BC implant (containing 17% cellulose) higher than that of autologous cartilage and lower than that of Gore-Tex implant via assessment of inflammatory and fibrotic reactions, necrosis, and fibrosis. Overall, the minimal foreign body response elicited by BC implants when implanted in rabbits, combined with their excellent mechanical properties, make it a suitable candidate for auricular (nose and trachea) cartilage reconstruction [165]. When implanted subcutaneously in rats, a novel BC wound dressing containing polyhexamethylene biguanide, an antimicrobial agent, and sericin was found to evoke a lower inflammatory response than the commercially available wound dressing [166]. Not only was it safer for *in vivo* use, but it also had higher clinical efficacy as demonstrated by significantly smaller wound size and higher extent of collagen formation. Like graphene and CNTs, the type and severity of cytotoxic effects of CNCs have been found to depend on its physicochemical properties such as size and surface charge as well as the form in which it is administered, *i.e.*, ingestion of liquid or gel formulation or inhalation of aerosolized particles. The toxicological implications of nanocellulose, particularly CNFs, may not be as severe as those of graphene and CNTs, more comprehensive *in vivo* studies are needed to fully realize the clinical potential of nanocellulose-based tissue engineering scaffolds.

### 4.4 Biodegradation

*In vitro* biodegradation of non-toxic and biocompatible PLA/CNF scaffolds, evaluated over 8 weeks in a phosphate-buffered saline medium at 37 °C, demonstrated that reinforcement with increased CNF content resisted the biodegradation of the composites and accelerated their wound healing potential [171]. An antibacterial nanocomposite of oxidized BC, chitosan and collagen, was found superior to commercial oxidized regenerated cellulose (ORC, also called Surgicel gauze) in its hemostatic capability and *in vivo* biodegradability, when tested in rat liver injury model [172]. It degraded faster than ORC and exhibited better procoagulant and blood clotting properties, in other words, faster hemostasis. Another study compared the degradation behavior of BC wound healing membranes (BC alone, not a composite) with Surgicel and found that both oxidized and non-oxidized versions of BC had

significantly lower degradation rate (< 10% vs > 45% after 60 days) than Surgicel [170]. Bacterial cellulose can be used to engineer both hard (bone and dental) and soft (nerve and skin) tissues. Crystallinity, molecular weight, hydrophilicity, and the type of chemical modification of BC-based materials are the four main factors that impact the *in vivo* biodegradation, which occurs via four major mechanisms, including hydrolysis, oxidation, enzymatic and physical degradation [173]. A recent study used enzyme (cellulase) encapsulation to control the *in vitro*/*in vivo* degradation kinetics of 3D printed CNF/chitosan hydrogel scaffolds [174].

## 5 Summary and future perspectives

Utilization of graphene, CNTs and nanocellulose for tissue engineering applications has come a long way and has indeed shown immense potential. These nanomaterials are particularly useful as reinforcing fillers or biocompatible coatings that enhance the mechanical and electrical properties of different natural and synthetic polymers, such that the composite matrices can be applied as tissue engineering scaffolds. However, there is still a long way to go before clinical translation of these nanomaterials for tissue engineering applications takes place. To do that, major limitations that need to be overcome are as follows: (a) lack of sufficient *in vivo* biodegradability data, (b) strategies to tune the rate of scaffold degradation such that it matches the rate of regeneration of the target tissue, (c) lack of sufficient *in vivo* toxicological data, (d) evaluating if *in vitro* tissue regeneration capabilities can be replicated *in vivo*, and (e) strategies to reduce foreign body reaction to implanted tissue engineering scaffolds containing these nanomaterials.

Based on the literature so far, cytotoxicity can be an issue, particularly in the case of CNTs and graphene. Cytotoxicity majorly depends on the physicochemical properties of the nanomaterial such as size, shape, composition, surface charge, quantity of impurities it contains, type of surface modification or functionalization (chemical or biological molecules), and most importantly, the concentration of nanomaterial used in the scaffold. By tuning these parameters, cytotoxicity of these nanomaterials can be mitigated. Incorporating bioactive compounds, e.g., peptides and growth factors, and encapsulating stem cells, in nanocomposite scaffolds to improve their tissue regeneration capability is an area that has only recently gained traction. So far, these strategies have proven effective in enhancing cell attachment and proliferation and achieving targeted cell differentiation. More research needs to be undertaken in this area to fully realize the commercial potential of graphene, CNTs and nanocellulose in the field of tissue engineering.

**Acknowledgements** This work was supported in part by the Center for Advanced Surface Engineering (CASE) under the National Science Foundation (NSF) Grant Number OIA-1457888 and the Arkansas EPSCoR program, ASSET III, Arkansas Biosciences Institute (ABI), and University of Arkansas College of Engineering Research & Innovation Seed Funding (ERISF). Also, this work was supported in part by the National Research Foundation of Korea (NRF) grants funded by the Korean government (NRF-2021R1A4A3025206 and NRF-2019M3A9H1103737).

## Declarations

**Conflict of interest** All authors declare that they have no conflict of interest.

**Ethical statement** There are no animal experiments carried out for this article.

## References

- Shadjou N, Hasanzadeh M. Graphene and its nanostructure derivatives for use in bone tissue engineering: Recent advances. *J Biomed Mater Res A*. 2016;104:1250–75.
- Shadjou N, Hasanzadeh M, Khalilzadeh B. Graphene based scaffolds on bone tissue engineering. *Bioengineered*. 2018;9:38–47.
- Sinha A, Sakon J, Roper DK, Li WJ, Ghosh A, Han HW, et al. Nanoscale particles and multifunctional hybrid soft nanomaterials in bio/nanomedicine. In: Kim JW, Roper DK, Li WJ, editors. *Soft matter and biomaterials on the nanoscale*. Singapore: World Scientific Publishing; 2020. p. 1–58.
- Eivazzadeh-Keihan R, Maleki A, de la Guardia M, Bani MS, Chenab KK, Pashazadeh-Panahi P, et al. Carbon based nanomaterials for tissue engineering of bone: Building new bone on small black scaffolds: A review. *J Adv Res*. 2019;18:185–201.
- Ku SH, Lee M, Park CB. Carbon-based nanomaterials for tissue engineering. *Adv Healthc Mater*. 2013;2:244–60.
- Khademhosseini A, Vacanti JP, Langer R. Progress in tissue engineering. *Sci Am*. 2009;300:64–71.
- Freed LE, Vunjak-Novakovic G, Biron RJ, Eagles DB, Lesnoy DC, Barlow SK, et al. Biodegradable polymer scaffolds for tissue engineering. *Biotechnology (NY)*. 1994;12:689–93.
- Tamayol A, Akbari M, Annabi N, Paul A, Khademhosseini A, Juncker D. Fiber-based tissue engineering: Progress, challenges, and opportunities. *Biotechnol Adv*. 2013;31:669–87.
- Shin SR, Li YC, Jang HL, Khoshakhlagh P, Akbari M, Nasajpour A, et al. Graphene-based materials for tissue engineering. *Adv Drug Deliv Rev*. 2016;105:255–74.
- Dugan JM, Gough JE, Eichhorn SJ. Bacterial cellulose scaffolds and cellulose nanowhiskers for tissue engineering. *Nanomedicine*. 2013;8:287–98.
- Domingues RMA, Gomes ME, Reis RL. The potential of cellulose nanocrystals in tissue engineering strategies. *Biomacromol*. 2014;15:2327–46.
- Kim HN, Jiao A, Hwang NS, Kim MS, Kang DH, Kim DH, et al. Nanotopography-guided tissue engineering and regenerative medicine. *Adv Drug Deliv Rev*. 2013;65:536–58.
- Shao Y, Fu J. Integrated micro/nanoengineered functional biomaterials for cell mechanics and mechanobiology: a materials perspective. *Adv Mater*. 2014;26:1494–533.
- Kim J, Kim HN, Lang Y, Pandit A. Biologically inspired micro- and nanoengineering systems for functional and complex tissues. *Tissue Eng Part A*. 2014;20:2127–30.

15. Park S, Choi KS, Kim D, Kim W, Lee D, Kim HN, et al. Controlled extracellular topographical and chemical cues for acceleration of neuronal development. *J Ind Eng Chem.* 2018;61:65–70.
16. Seonwoo H, Bae WG, Park S, Kim HN, Choi KS, Lim KT, Hyun H, et al. Hierarchically micro-and nanopatterned topographical cues for modulation of cellular structure and function. *IEEE Trans Nanobioscience.* 2016;15:835–42.
17. Stoppel WL, Kaplan DL, Black LD. Electrical and mechanical stimulation of cardiac cells and tissue constructs. *Adv Drug Deliv Rev.* 2016;96:135–55.
18. Coppens SR, Fukushima S, Shintani Y, Takahashi K, Varela-Carver A, Salem H, et al. A factor underlying late-phase arrhythmogenicity after cell therapy to the heart: Global downregulation of connexin43 in the host myocardium after skeletal myoblast transplantation. *Circulation* 2008;118:S138–44.
19. Lekshmi G, Sana SS, Nguyen VH, Nguyen THC, Nguyen CC, Le QV, et al. Recent progress in carbon nanotube polymer composites in tissue engineering and regeneration. *Int J Mol Sci.* 2020;21:6440.
20. Kroto HW, Heath JR, O'Brien SC, Curl RF, Smalley RE. C60: Buckminsterfullerene. *Nature.* 1985;318:162–3.
21. Iijima S. Helical microtubules of graphitic carbon. *Nature.* 1991;354:56–8.
22. Patil TV, Patel DK, Dutta SD, Ganguly K, Santra TS, Lim KT. Nanocellulose, a versatile platform: From the delivery of active molecules to tissue engineering applications. *Bioact Mater.* 2022;9:566–89.
23. Patel KD, Singh RK, Kim HW. Carbon-based nanomaterials as an emerging platform for theranostics. *Mater Horiz.* 2019;6:434–69.
24. Luo H, Cha R, Li J, Hao W, Zhang Y, Zhou F. Advances in tissue engineering of nanocellulose-based scaffolds: A review. *Carbohydr Polym* 2019;224:115144.
25. Maiti D, Tong X, Mou X, Yang K. Carbon-based nanomaterials for biomedical applications: a recent study. *Front Pharmacol.* 2019;9:1401.
26. Cha C, Shin SR, Annabi N, Dokmeci MR, Khademhosseini A. Carbon-based nanomaterials: Multifunctional materials for biomedical engineering. *ACS Nano.* 2013;7:2891–7.
27. Bacakova L, Pajorova J, Bacakova M, Skogberg A, Kallio P, Kolarova K, et al. Versatile application of nanocellulose: from industry to skin tissue engineering and wound healing. *Nanomaterials (Basel).* 2019;9:164.
28. Novoselov KS, Geim AK, Morozov S v., Morozov SV, Jiang D, Zhang Y, Dubonos SV, et al. Electric field in atomically thin carbon films. *Science.* 2004;306:666–9.
29. Geim AK, Novoselov KS. The rise of graphene. *Nanosci Technol A Collection Rev Nat J.* 2009. [https://doi.org/10.1142/9789814287005\\_0002](https://doi.org/10.1142/9789814287005_0002).
30. Tiwari SK, Sahoo S, Wang N, Huczko A. Graphene research and their outputs: Status and prospect. *J Sci Adv Mater Devices.* 2020;5:10–29.
31. Geim AK. Graphene: Status and prospects. *Science.* 2009;324:1530–34.
32. Goenka S, Sant V, Sant S. Graphene-based nanomaterials for drug delivery and tissue engineering. *J Control Release.* 2014;173:75–88.
33. Mena F, Abdelghani A, Mena B. Graphene nanomaterials as biocompatible and conductive scaffolds for stem cells: impact for tissue engineering and regenerative medicine. *J Tissue Eng Regen Med.* 2015;9:1321–38.
34. Geetha Bai R, Ninan N, Muthoosamy K, Manickam S. Graphene: A versatile platform for nanotheranostics and tissue engineering. *Prog Mater Sci.* 2018;91:24–69.
35. Engler AJ, Sen S, Sweeney HL, Discher DE. Matrix elasticity directs stem cell lineage specification. *Cell.* 2006;126:677–89.
36. Li N, Zhang Q, Gao S, Song Q, Huang R, Wang L. Three-dimensional graphene foam as a biocompatible and conductive scaffold for neural stem cells. *Sci Rep.* 2013;3:1604.
37. Krueger E, Chang AN, Brown D, Eixenberger J, Brown R, Rastegar S, et al. Graphene foam as a three-dimensional platform for myotube growth. *ACS Biomater Sci Eng.* 2016;2:1234–41.
38. Yocham KM, Scott C, Fujimoto K, Brown R, Tanasse E, Oxford JT, et al. Mechanical properties of graphene foam and graphene foam—tissue composites. *Adv Eng Mater.* 2018;20:1800166.
39. Huang Q, Cai Y, Yang X, Li W, Pu H, Liu Z, et al. Graphene foam/hydrogel scaffolds for regeneration of peripheral nerve using ADSCs in a diabetic mouse model. *Nano Res.* 2021;15:3434–45.
40. Zhang L, Wang Z, Xu C, Li Y, Gao J, Wang W, et al. High strength graphene oxide/polyvinyl alcohol composite hydrogels. *J Mater Chem.* 2011;21:10399–406.
41. Zhou K, Yu P, Shi X, Ling T, Zeng W, Chen A, et al. Hierarchically porous hydroxyapatite hybrid scaffold incorporated with reduced graphene oxide for rapid bone ingrowth and repair. *ACS Nano.* 2019;13:9595–606.
42. Huang Q, Cai Y, Zhang X, Liu J, Liu Z, Li B, et al. Aligned graphene mesh-supported double network natural hydrogel conduit loaded with netrin-1 for peripheral nerve regeneration. *ACS Appl Mater Interfaces.* 2021;13:112–22.
43. Choe G, Kim SW, Park J, Park J, Kim S, Kim YS, et al. Antioxidant activity reinforced reduced graphene oxide/alginate microgels: Mesenchymal stem cell encapsulation and regeneration of infarcted hearts. *Biomaterials* 2019;225:119513.
44. Du Y, Ge J, Li Y, Ma PX, Lei B. Biomimetic elastomeric, conductive and biodegradable polycitrate-based nanocomposites for guiding myogenic differentiation and skeletal muscle regeneration. *Biomaterials.* 2018;157:40–50.
45. Yoon OJ, Jung CY, Sohn IY, Kim HJ, Hong B, Jhon MS, et al. Nanocomposite nanofibers of poly(D, L-lactic-co-glycolic acid) and graphene oxide nanosheets. *Compos Part A Appl Sci Manuf.* 2011;42:1978–84.
46. Liu S, Zhou C, Mou S, Li J, Zhou M, Zeng Y, Li J, Zhou M, Zeng Y, et al. Biocompatible graphene oxide–collagen composite aerogel for enhanced stiffness and in situ bone regeneration. *Mater Sci Eng C Mater Biol Appl.* 2019;105:110137.
47. Zheng Z, Chen Y, Hong H, Shen Y, Wang Y, Sun J, et al. The “Yin and Yang” of immunomodulatory magnesium-enriched graphene oxide nanoscrolls decorated biomimetic scaffolds in promoting bone regeneration. *Adv Healthc Mater.* 2021;10:e2000631.
48. Park J, Kim YS, Ryu S, Kang WS, Park S, Han J, et al. Graphene potentiates the myocardial repair efficacy of mesenchymal stem cells by stimulating the expression of angiogenic growth factors and gap junction protein. *Adv Funct Mater.* 2015;25:2590–600.
49. Jiao D, Zheng A, Liu Y, Zhang X, Wang X, Wu J, et al. Bidirectional differentiation of BMSCs induced by a biomimetic procallus based on a gelatin-reduced graphene oxide reinforced hydrogel for rapid bone regeneration. *Bioact Mater.* 2021;6:2011–28.
50. Park S, Kim H, Choi KS, Ji MK, Kim S, Gwon Y, et al. Graphene-Chitosan hybrid dental implants with enhanced antibacterial and cell-proliferation properties. *Appl Sci.* 2020;10:4888.
51. Paul A, Hasan A, Kindi HA, Gaharwar AK, Rao VT, Nikkhah M, et al. Injectable graphene oxide/hydrogel-based angiogenic gene delivery system for vasculogenesis and cardiac repair. *ACS Nano* 2014;8:8050–8062.

52. Chen GY, Pang DWP, Hwang SM, Tuan HY, Hu YC. A graphene-based platform for induced pluripotent stem cells culture and differentiation. *Biomaterials*. 2012;33:418–27.
53. Kalbacova M, Broz A, Kong J, Kalbac M. Graphene substrates promote adherence of human osteoblasts and mesenchymal stromal cells. *Carbon N Y*. 2010;48:4323–9.
54. Nayak TR, Andersen H, Makam VS, Khaw C, Bae S, Xu X, et al. Graphene for controlled and accelerated osteogenic differentiation of human mesenchymal stem cells. *ACS Nano*. 2011;5:4670–8.
55. Lee WC, Lim CH, Shi H, Tang LA, Wang Y, Lim CT, et al. Origin of enhanced stem cell growth and differentiation on graphene and graphene oxide. *ACS Nano*. 2011;5:7334–41.
56. Weaver CL, Cui XT. Directed neural stem cell differentiation with a functionalized graphene oxide nanocomposite. *Adv Healthc Mater*. 2015;4:1408–16.
57. Kim J, Choi KS, Kim Y, Lim KT, Seonwoo H, Park Y, et al. Bioactive effects of graphene oxide cell culture substratum on structure and function of human adipose-derived stem cells. *J Biomed Mater Res A*. 2013;101:3520–30.
58. Luong-Van EK, Madanagopal TT, Rosa V. Mechanisms of graphene influence on cell differentiation. *Mater Today Chem* 2020;16:100250.
59. Li Y, Liu Y, Fu Y, Wei T, Le Guyader L, Gao G, et al. The triggering of apoptosis in macrophages by pristine graphene through the MAPK and TGF-beta signaling pathways. *Biomaterials*. 2012;33:402–11.
60. Sasidharan A, Panchakarla LS, Chandran P, Menon D, Nair S, Rao CN, et al. Differential nano-bio interactions and toxicity effects of pristine versus functionalized graphene. *Nanoscale*. 2011;3:2461–4.
61. Chang Y, Yang ST, Liu JH, Dong E, Wang Y, Cao A, et al. In vitro toxicity evaluation of graphene oxide on A549 cells. *Toxicol Lett*. 2011;200:201–10.
62. Zhang Y, Ali SF, Dervishi E, Xu Y, Li Z, Casciano D, et al. Cytotoxicity effects of graphene and single-wall carbon nanotubes in neural pheochromocytoma-derived PC12 cells. *ACS Nano*. 2010;4:3181–6.
63. Wang K, Ruan J, Song H, Zhang J, Wo Y, Guo S, et al. Biocompatibility of graphene oxide. *Nanoscale Res Lett*. 2011;6:8.
64. Figarol A, Pourchez J, Boudard D, Forest V, Akono C, Tulliani JM, et al. In vitro toxicity of carbon nanotubes, nano-graphite and carbon black, similar impacts of acid functionalization. *Toxicol In Vitro*. 2015;30:476–85.
65. Zhang Q, Liu X, Meng H, Liu S, Zhang C. Reduction pathway-dependent cytotoxicity of reduced graphene oxide. *Environ Sci Nano*. 2018;5:1361–71.
66. Cebadero-Domínguez O, Ferrández-Gómez B, Sánchez-Ballester S, Moreno J, Jos A, Cameán AM. In vitro toxicity evaluation of graphene oxide and reduced graphene oxide on Caco-2 cells. *Toxicol Rep*. 2022;9:1130–8.
67. Ezzati N, Mahjoub AR, Shokrollahi S, Amiri A, Abolhosseini Shahrnoy A. Novel biocompatible amino acids-functionalized three-dimensional graphene foams: as the attractive and promising cisplatin carriers for sustained release goals. *Int J Pharm* 2020;589:119857.
68. Zhang W, Yan L, Li M, Zhao R, Yang X, Ji T, et al. Deciphering the underlying mechanisms of oxidation-state dependent cytotoxicity of graphene oxide on mammalian cells. *Toxicol Lett*. 2015;237:61–71.
69. Xing W, Lalwani G, Rusakova I, et al. Degradation of graphene by hydrogen peroxide. *Part Part Syst Charact*. 2014;31:745–50.
70. Kotchey GP, Allen BL, Vedala H, Yanamala N, Kapralov AA, Tyurina YY, et al. The enzymatic oxidation of graphene oxide. *ACS Nano*. 2011;5:2098–108.
71. Spitalsky Z, Tasis D, Papagelis K, Galiotis C. Carbon nanotube-polymer composites: Chemistry, processing, mechanical and electrical properties. *Prog Polym Sci*. 2010;35:357–401.
72. Gorain B, Choudhury H, Pandey M, Kesharwani P, Abeer MM, Tekade RK, et al. Carbon nanotube scaffolds as emerging nanoplatform for myocardial tissue regeneration: A review of recent developments and therapeutic implications. *Biomed Pharmacother*. 2018;104:496–508.
73. Raphey VR, Henna TK, Nivitha KP, Mufeedha P, Sabu C, Pramod K. Advanced biomedical applications of carbon nanotube. *Mater Sci Eng C Mater Biol Appl*. 2019;100:616–30.
74. Saliev T. The advances in biomedical applications of carbon nanotubes. *J Carbon Res*. 2019;5:29.
75. Veetil JV, Ye K. Tailored carbon nanotubes for tissue engineering applications. *Biotechnol Prog*. 2009;25:709–21.
76. Elhissi AMA, Ahmed W, Hassan IU, Dhanak VR, D’Emanuele A. Carbon nanotubes in cancer therapy and drug delivery. *J Drug Deliv* 2012;2012:837327.
77. Ackermann J, Metternich JT, Herbertz S, Kruss S. Biosensing with fluorescent carbon nanotubes. *Angew Chem Int Ed Engl*. 2022;61:e202112372.
78. Zhao J, Zhong D, Zhou S. NIR-I-to-NIR-II fluorescent nanomaterials for biomedical imaging and cancer therapy. *J Mater Chem B*. 2018;6:349–65.
79. Yudasaka M, Yomogida Y, Zhang M, Tanaka T, Nakahara M, Kobayashi N, et al. Near-infrared photoluminescent carbon nanotubes for imaging of brown fat. *Sci Rep*. 2017;7:44760.
80. de la Zerda A, Kim JW, Galanzha EI, Gambhir SS, Zharov VP. Advanced contrast nanoagents for photoacoustic molecular imaging, cytometry, blood test and photothermal theranostics. *Contrast Media Mol Imaging*. 2011;6:346–69.
81. Galanzha EI, Shashkov EV, Kelly T, Kim JW, Yang L, Zharov VP. In vivo magnetic enrichment and multiplex photoacoustic detection of circulating tumour cells. *Nat Nanotechnol*. 2009;4:855–860.
82. Hopley EL, Salmasi S, Kalaskar DM, Seifalian AM. Carbon nanotubes leading the way forward in new generation 3D tissue engineering. *Biotechnol Adv*. 2014;32:1000–14.
83. Huang B. Carbon nanotubes and their polymeric composites: the applications in tissue engineering. *Biomanuf Rev*. 2020;5:3.
84. Kotagiri N, Kim JW. Stealth nanotubes: strategies of shielding carbon nanotubes to evade opsonization and improve biodistribution. *Int J Nanomedicine*. 2014;9:85–105.
85. Kotagiri N, Lee JS, Kim JW. Selective pathogen targeting and macrophage evading carbon nanotubes through dextran sulfate coating and PEGylation for photothermal theranostics. *J Biomed Nanotechnol*. 2013;9:1008–16.
86. Kotagiri N, Kim JW. Carbon nanotubes Fed on “Carbs”: Coating of single-walled carbon nanotubes by dextran sulfate. *Macromol Biosci*. 2010;10:231–8.
87. Zharov VP, Galanzha EI, Shashkov EV, Kim JW, Khlebtsov NG, Tuchin VV. Photoacoustic flow cytometry: principle and application for real-time detection of circulating single nanoparticles, pathogens, and contrast dyes in vivo. *J Biomed Opt*. 2007;12:051503.
88. Zharov VP, Kim JW, Curiel DT, Kim JW, Curiel DT, Everts M. Self-assembling nanoclusters in living systems: application for integrated photothermal nanodiagnosics and nanotherapy. *Nanomedicine*. 2005;1:326–45.
89. Kim JW, Shashkov EV, Galanzha EI, Kotagiri N, Zharov VP. Photothermal antimicrobial nanotherapy and nanodiagnosics with self-assembling carbon nanotube clusters. *Lasers Surg Med* 2007;39:622–34.
90. Kim JW, Galanzha EI, Zaharoff DA, Griffin RJ, Zharov VP. Nanotheranostics of circulating tumor cells, infections and other pathological features in vivo. *Mol Pharm*. 2013;10:813–30.

91. Kim JW, Galanzha EI, Shashkov EV, Moon HM, Zharov VP. Golden carbon nanotubes as multimodal photoacoustic and photothermal high-contrast molecular agents. *Nat Nanotechnol.* 2009;4:688–94.
92. Zhao G, Zhang X, Li B, Huang G, Xu F, Zhang X. Solvent-free fabrication of carbon nanotube/silk fibroin electrospun matrices for enhancing cardiomyocyte functionalities. *ACS Biomater Sci Eng.* 2020;6:1630–40.
93. Park S, Park J, Jo I, Cho SP, Sung D, Ryu S, et al. In situ hybridization of carbon nanotubes with bacterial cellulose for three-dimensional hybrid bioscaffolds. *Biomaterials.* 2015;58:93–102.
94. Wang L, Liu Y, Ye G, He Y, Li B, Guan Y, et al. Injectable and conductive cardiac patches repair infarcted myocardium in rats and minipigs. *Nat Biomed Eng.* 2021;5:1157–73.
95. Ghosh S, Haldar S, Gupta S, Bisht A, Chauhan S, Kumar V, et al. Anisotropically conductive biodegradable scaffold with coaxially aligned carbon nanotubes for directional regeneration of peripheral nerves. *ACS Appl Bio Mater.* 2020;3:5796–812.
96. Xu Y, Hirata E, Iizumi Y, Ushijima N, Kubota K, Kimura S, et al. Single-walled carbon nanotube membranes accelerate active osteogenesis in bone defects: potential of guided bone regeneration membranes. *ACS Biomater Sci Eng.* 2022;8:1667–75.
97. Bahrami Miyajani P, Semnani D, Hossein Ravandi A, Karbasi S, Fakhrali A, Mohammadi S. Fabrication and characterization of chitosan-gelatin/single-walled carbon nanotubes electrospun composite scaffolds for cartilage tissue engineering applications. *Polym Adv Technol.* 2022;33:81–95.
98. Gan Z, Zhao Y, Wu Y, Yang W, Zhao Z, Zhao L. Three-dimensional, biomimetic electrospun scaffolds reinforced with carbon nanotubes for temporomandibular joint disc regeneration. *Acta Biomater.* 2022;147:221–34.
99. Kunisaki A, Kodama A, Ishikawa M, Ueda T, Lima MD, Kondo T, et al. Carbon-nanotube yarns induce axonal regeneration in peripheral nerve defect. *Sci Rep.* 2021;11:19562.
100. Patel KD, Kim TH, Lee EJ, Han CM, Lee JY, Singh RK, et al. Nanostructured biointerfacing of metals with carbon nanotube/chitosan hybrids by electrodeposition for cell stimulation and therapeutics delivery. *ACS Appl Mater Interfaces.* 2014;6:20214–24.
101. Patel KD, Kim TH, Mandakhyar N, Singh RK, Jang JH, Lee JH, et al. Coating biopolymer nanofibers with carbon nanotubes accelerates tissue healing and bone regeneration through orchestrated cell- and tissue-regulatory responses. *Acta Biomater.* 2020;108:97–110.
102. Patel DK, Dutta SD, Ganguly K, Kim JW, Lim KT. Enhanced osteogenic potential of unzipped carbon nanotubes for tissue engineering. *J Biomed Mater Res A.* 2021;109:1869–80.
103. Das K, Madhusoodan AP, Mili B, Kumar A, Saxena AC, Kumar K, et al. Functionalized carbon nanotubes as suitable scaffold materials for proliferation and differentiation of canine mesenchymal stem cells. *Int J Nanomedicine.* 2017;12:3235–52.
104. Imaninezhad M, Schober J, Griggs D, Ruminski P, Kuljanishvili I, Zustiak SP. Cell attachment and spreading on carbon nanotubes is facilitated by integrin binding. *Front Bioeng Biotechnol.* 2018;6:129.
105. Saleemi MA, Hosseini Fouladi M, Yong PVC, Chinna K, Palanisamy NK, Wong EH. Toxicity of carbon nanotubes: Molecular mechanisms, signaling cascades, and remedies in biomedical applications. *Chem Res Toxicol.* 2021;34:24–46.
106. Dong J, Ma Q. Suppression of basal and carbon nanotube-induced oxidative stress, inflammation and fibrosis in mouse lungs by Nrf2. *Nanotoxicology.* 2016;10:699–709.
107. Garibaldi S, Brunelli C, Bavastrello V, Ghigliotti G, Nicolini C. Carbon nanotube biocompatibility with cardiac muscle cells. *Nanotechnology.* 2006;17:391.
108. Kalbacova M, Kalbac M, Dunsch L, Kataura H, Hempel U. The study of the interaction of human mesenchymal stem cells and monocytes/macrophages with single-walled carbon nanotube films. *Phys Status Solidi B Basic Solid State Phys.* 2006;243:3514–8.
109. Manna SK, Sarkar S, Barr J, Wise K, Barrera EV, Jejelowo O, et al. Single-walled carbon nanotube induces oxidative stress and activates nuclear transcription factor- $\kappa$ B in human keratinocytes. *Nano Lett.* 2005;5:1676–84.
110. Davoren M, Herzog E, Casey A, Cottineau B, Chambers G, Byrne HJ, et al. In vitro toxicity evaluation of single walled carbon nanotubes on human A549 lung cells. *Toxicol In Vitro.* 2007;21:438–48.
111. Casey A, Herzog E, Lyng FM, Byrne HJ, Chambers G, Davoren M. Single walled carbon nanotubes induce indirect cytotoxicity by medium depletion in A549 lung cells. *Toxicol Lett.* 2008;179:78–84.
112. Xu H, Bai J, Meng J, Hao W, Xu H, Cao JM. Multi-walled carbon nanotubes suppress potassium channel activities in PC12 cells. *Nanotechnology.* 2009;20:285102.
113. Ye SF, Wu YH, Hou ZQ, Zhang QQ. ROS and NF- $\kappa$ B are involved in upregulation of IL-8 in A549 cells exposed to multi-walled carbon nanotubes. *Biochem Biophys Res Commun.* 2009;379:643–8.
114. Magrez A, Kasas S, Salicio V, Pasquier N, Seo JW, Celio M, et al. Cellular toxicity of carbon-based nanomaterials. *Nano Lett.* 2006;6:1121–5.
115. Monteiro-Riviere NA, Nemanich RJ, Inman AO, Wang YY, Riviere JE. Multi-walled carbon nanotube interactions with human epidermal keratinocytes. *Toxicol Lett.* 2005;155:377–84.
116. Zhu L, Chang DW, Dai L, Hong Y. DNA damage induced by multiwalled carbon nanotubes in mouse embryonic stem cells. *Nano Lett.* 2007;7:3592–7.
117. Zhou L, Forman HJ, Ge Y, Lunec J. Multi-walled carbon nanotubes: A cytotoxicity study in relation to functionalization, dose and dispersion. *Toxicol In Vitro.* 2017;42:292–8.
118. Kavosi A, Hosseini Ghale Noei S, Madani S, Khalighfar S, Khodayari S, Khodayari H, et al. The toxicity and therapeutic effects of single-and multi-wall carbon nanotubes on mice breast cancer. *Sci Rep* 2018;8:8375.
119. Murr LE, Garza KM, Soto KF, Carrasco A, Powell TG, Ramirez DA, et al. Cytotoxicity assessment of some carbon nanotubes and related carbon nanoparticle aggregates and the implications for anthropogenic carbon nanotube aggregates in the environment. *Int J Environ Res Public Health.* 2005;2:31–42.
120. Mooney E, Dockery P, Greiser U, Murphy M, Barron V. Carbon nanotubes and mesenchymal stem cells: Biocompatibility, proliferation and differentiation. *Nano Lett.* 2008;8:2137–43.
121. Kim HB, Jin B, Patel DK, Kim JW, Kim J, Seonwoo H, et al. Enhanced osteogenesis of human mesenchymal stem cells in presence of single-walled carbon nanotubes. *IEEE Trans Nanobioscience.* 2019;18:463–8.
122. Li R, Wang X, Ji Z, Sun B, Zhang H, Chang CH, et al. Surface charge and cellular processing of covalently functionalized multiwall carbon nanotubes determine pulmonary toxicity. *ACS Nano.* 2013;7:2352–68.
123. Wan B, Wang ZX, Lv QY, Dong PX, Zhao LX, Yang Y, et al. Single-walled carbon nanotubes and graphene oxides induce autophagosome accumulation and lysosome impairment in primarily cultured murine peritoneal macrophages. *Toxicol Lett.* 2013;221:118–27.
124. Modugno G, Ksar F, Battigelli A, Russier J, Lonchambon P, da Silva EE, et al. A comparative study on the enzymatic

- biodegradability of covalently functionalized double- and multi-walled carbon nanotubes. *Carbon* N Y. 2016;100:367–74.
125. Seo YR, Kim JW, Hoon S, Kim J, Chung JH, Lim KT, et al. Cellulose-based nanocrystals: Sources and applications via agricultural byproducts. *J Biosyst Eng*. 2018;43:59–71.
  126. Mohammadinejad R, Karimi S, Irvani S, Varma RS. Plant-derived nanostructures: types and applications. *Green Chem*. 2015;18:20–52.
  127. Rajan K, Djioleu A, Kandhola G, Labbé N, Sakon J, Carrier DJ, et al. Investigating the effects of hemicellulose pre-extraction on the production and characterization of loblolly pine nanocellulose. *Cellulose*. 2020;27:3693–706.
  128. Kandhola G, Djioleu A, Rajan K, Labbé N, Sakon J, Carrier DJ, et al. Maximizing production of cellulose nanocrystals and nanofibers from pre-extracted loblolly pine kraft pulp: a response surface approach. *Bioresour Bioprocess*. 2020;7:1–16.
  129. Kandhola G, Djioleu A, Rajan K, Batta-Mpouma J, Labbé N, Sakon J, et al. Impact of species-based wood feedstock variability on physicochemical properties of cellulose nanocrystals. *Cellulose*. 2022;29:8213–28.
  130. Lin N, Dufresne A. Nanocellulose in biomedicine: Current status and future prospect. *Eur Polym J*. 2014;59:302–25.
  131. Tortorella S, Vetri Buratti V, Maturi M, Sambri L, Comes Franchini M, Locatelli E. Surface-modified nanocellulose for application in biomedical engineering and nanomedicine: a review. *Int J Nanomedicine*. 2020;15:9909–37.
  132. Batta-Mpouma J, Kandhola G, Sakon J, Kim JW. Covalent crosslinking of colloidal cellulose nanocrystals for multifunctional nanostructured hydrogels with tunable physicochemical properties. *Biomacromolecules*. 2022;23:4085–96.
  133. Habibi Y, Lucia LA, Rojas OJ. Cellulose nanocrystals: Chemistry, self-assembly, and applications. *Chem Rev*. 2010;110:3479–500.
  134. Sinha A, Martin EM, Lim KT, Carrier DJ, Han H, Kim JW. Cellulose nanocrystals as advanced “Green” materials for biological and biomedical engineering. *J Biosyst Eng*. 2015;40:373–93.
  135. Kaur P, Sharma N, Munagala M, Rajkhowa R, Aallardyce B, Shastri Y, et al. Nanocellulose: Resources, physio-chemical properties, current uses and future applications. *Front Nanotechnol*. 2021;3:747329.
  136. Wang J, Tavakoli J, Tang Y. Bacterial cellulose production, properties and applications with different culture methods—A review. *Carbohydr Polym*. 2019;219:63–76.
  137. Stumpf TR, Yang X, Zhang J, Cao X. In situ and ex situ modifications of bacterial cellulose for applications in tissue engineering. *Mater Sci Eng C Mater Biol Appl*. 2018;82:372–83.
  138. Domingues RMA, Chiera S, Gershovich P, Motta A, Reis RL, Gomes ME. Enhancing the biomechanical performance of anisotropic nanofibrous scaffolds in tendon tissue engineering: reinforcement with cellulose nanocrystals. *Adv Healthc Mater*. 2016;5:1364–75.
  139. Dutta SD, Patel DK, Seo YR, Park CW, Lee SH, Kim JW, et al. In vitro biocompatibility of electrospun poly( $\epsilon$ -caprolactone)/cellulose nanocrystals-nanofibers for tissue engineering. *J Nanomater*. 2019;2019:2061545.
  140. Joshi MK, Tiwari AP, Pant HR, Shrestha BK, Kim HJ, Park CH, et al. In situ generation of cellulose nanocrystals in polycaprolactone nanofibers: effects on crystallinity, mechanical strength, biocompatibility, and biomimetic mineralization. *ACS Appl Mater Interfaces*. 2015;7:19672–83.
  141. Huang A, Peng X, Geng L, Zhang L, Huang K, Chen B, et al. Electrospun poly (butylene succinate)/cellulose nanocrystals bio-nanocomposite scaffolds for tissue engineering: Preparation, characterization and in vitro evaluation. *Polym Test*. 2018;71:101–9.
  142. He X, Xiao Q, Lu C, Wang Y, Zhang X, Zhao J, et al. Uniaxially aligned electrospun all-cellulose nanocomposite nanofibers reinforced with cellulose nanocrystals: Scaffold for tissue engineering. *Biomacromolecules*. 2014;15:618–27.
  143. Mo Y, Guo R, Liu J, Lan Y, Zhang Y, Xue W, et al. Preparation and properties of PLGA nanofiber membranes reinforced with cellulose nanocrystals. *Colloids Surf B Biointerfaces*. 2015;132:177–84.
  144. Amaral HR, Wilson JA, do Amaral RJFC, Pasçu I, de Oliveira FCS, Kearney CJ, et al. Synthesis of bilayer films from regenerated cellulose nanofibers and poly(globalide) for skin tissue engineering applications. *Carbohydr Polym* 2021;252:117201.
  145. Patel DK, Dutta SD, Hexiu J, Ganguly K, Lim KT. Bioactive electrospun nanocomposite scaffolds of poly(lactic acid)/cellulose nanocrystals for bone tissue engineering. *Int J Biol Macromol*. 2020;162:1429–41.
  146. Shi Q, Guo W, Terrell L, Qureshi AT, Hayes DJ, et al. Electrospun bio-nanocomposite scaffolds for bone tissue engineering by cellulose nanocrystals reinforcing maleic anhydride grafted PLA. *ACS Appl Mater Interfaces*. 2013;5:3847–54.
  147. Zhang C, Salick MR, Cordie TM, Ellingham T, Dan Y, Turng LS. Incorporation of poly(ethylene glycol) grafted cellulose nanocrystals in poly(lactic acid) electrospun nanocomposite fibers as potential scaffolds for bone tissue engineering. *Mater Sci Eng C Mater Biol Appl*. 2015;49:463–71.
  148. Gorgieva S, Girandon L, Kokol V. Mineralization potential of cellulose-nanofibrils reinforced gelatine scaffolds for promoted calcium deposition by mesenchymal stem cells. *Mater Sci Eng C Mater Biol Appl*. 2017;73:478–89.
  149. Park M, Lee D, Shin S, Hyun J. Effect of negatively charged cellulose nanofibers on the dispersion of hydroxyapatite nanoparticles for scaffolds in bone tissue engineering. *Colloids Surf B Biointerfaces*. 2015;130:222–8.
  150. Doench I, Torres-Ramos MEW, Montebault A, Nunes de Oliveira P, Halimi C, Viguier E, et al. Injectable and gellable chitosan formulations filled with cellulose nanofibers for intervertebral disc tissue engineering. *Polymers (Basel)*. 2018;10:1202.
  151. Dutta SD, Hexiu J, Patel DK, Ganguly K, Lim KT. 3D-printed bioactive and biodegradable hydrogel scaffolds of alginate/gelatin/cellulose nanocrystals for tissue engineering. *Int J Biol Macromol*. 2021;167:644–58.
  152. Shaheen TI, Montaser AS, Li S. Effect of cellulose nanocrystals on scaffolds comprising chitosan, alginate and hydroxyapatite for bone tissue engineering. *Int J Biol Macromol*. 2019;121:814–21.
  153. Mohammadalipour M, Karbasi S, Behzad T, Mohammadalipour Z, Zamani M. Effect of cellulose nanofibers on polyhydroxybutyrate electrospun scaffold for bone tissue engineering applications. *Int J Biol Macromol*. 2022;220:1402–14.
  154. Naseri N, Poirier JM, Girandon L, Fröhlich M, Oksman K, Mathew AP. 3-Dimensional porous nanocomposite scaffolds based on cellulose nanofibers for cartilage tissue engineering: tailoring of porosity and mechanical performance. *RSC Adv*. 2016;6:5999–6007.
  155. Nasri-Nasrabadi B, Mehrasa M, Rafienia M, Bonakdar S, Behzad T, Gavanji S. Porous starch/cellulose nanofibers composite prepared by salt leaching technique for tissue engineering. *Carbohydr Polym*. 2014;108:232–8.
  156. Ghorbani M, Roshangar L, Soleimani Rad J. Development of reinforced chitosan/pectin scaffold by using the cellulose nanocrystals as nanofillers: An injectable hydrogel for tissue engineering. *Eur Polym J* 2020;130:109697.

157. Goudarzi ZM, Behzad T, Ghasemi-Mobarakeh L, Kharaziha M. An investigation into influence of acetylated cellulose nanofibers on properties of PCL/Gelatin electrospun nanofibrous scaffold for soft tissue engineering. *Polymer (Guildf)* 2021;213:123313.
158. Markstedt K, Mantas A, Tournier I, Martínez Ávila H, Hägg D, Gatenholm P. 3D bioprinting human chondrocytes with nanocellulose-alginate bioink for cartilage tissue engineering applications. *Biomacromolecules*. 2015;16:1489–96.
159. Ju J, Gu Z, Liu X, Zhang S, Peng X, Kuang T. Fabrication of bimodal open-porous poly (butylene succinate)/cellulose nanocrystals composite scaffolds for tissue engineering application. *Int J Biol Macromol*. 2020;147:1164–73.
160. Domingues RM, Silva M, Gershovich P, Betta S, Babo P, Caridade SG, et al. Development of injectable hyaluronic acid/cellulose nanocrystals bionanocomposite hydrogels for tissue engineering applications. *Bioconjug Chem*. 2015;26:1571–81.
161. Saska S, Teixeira LN, de Castro Raucchi LMS, Scarel-Caminaga RM, Franchi LP, Dos Santos RA, et al. Nanocellulose-collagen-apatite composite associated with osteogenic growth peptide for bone regeneration. *Int J Biol Macromol*. 2017;103:467–76.
162. Osorio M, Ortiz I, Gañán P, Naranjo T, Zuluaga R, van Kooten TG, et al. Novel surface modification of three-dimensional bacterial nanocellulose with cell-derived adhesion proteins for soft tissue engineering. *Mater Sci Eng C Mater Biol Appl*. 2019;100:697–705.
163. Vielreicher M, Kralisch D, Völkl S, Sternal F, Arkudas A, Friedrich O. Bacterial nanocellulose stimulates mesenchymal stem cell expansion and formation of stable collagen-I networks as a novel biomaterial in tissue engineering. *Sci Rep*. 2018;8:9401.
164. Stoudmann N, Schmutz M, Hirsch C, Nowack B, Som C. Human hazard potential of nanocellulose: quantitative insights from the literature. *Nanotoxicology*. 2020;14:1241–57.
165. Martínez Ávila H, Schwarz S, Feldmann EM, Mantas A, von Bomhard A, Gatenholm P, et al. Biocompatibility evaluation of densified bacterial nanocellulose hydrogel as an implant material for auricular cartilage regeneration. *Appl Microbiol Biotechnol*. 2014;98:7423–35.
166. Napavichayanun S, Yamdech R, Aramwit P. The safety and efficacy of bacterial nanocellulose wound dressing incorporating sericin and polyhexamethylene biguanide: in vitro, in vivo and clinical studies. *Arch Dermatol Res*. 2016;308:123–32.
167. Li J, Wang X, Chang CH, Jiang J, Liu Q, Liu X, et al. Nanocellulose length determines the differential cytotoxic effects and inflammatory responses in macrophages and hepatocytes. *Small*. 2021;17:e2102545.
168. Mahmoud KA, Mena JA, Male KB, Hrapovic S, Kamen A, Luong JH. Effect of surface charge on the cellular uptake and cytotoxicity of fluorescent labeled cellulose nanocrystals. *ACS Appl Mater Interfaces*. 2010;2:2924–32.
169. Nordli HR, Chinga-Carrasco G, Rokstad AM, Pukstad B. Producing ultrapure wood cellulose nanofibrils and evaluating the cytotoxicity using human skin cells. *Carbohydr Polym*. 2016;150:65–73.
170. Queirós EC, Pinheiro SP, Pereira JE, Prada J, Pires I, Dourado F, et al. Hemostatic dressings made of oxidized bacterial nanocellulose membranes. *Polysaccharides*. 2021;2:80–99.
171. Revati R, Majid MSA, Ridzuan MJM, Mamat N, Cheng EM, Alshahrani HA. In vitro biodegradation, cytotoxicity, and biocompatibility of polylactic acid/napiier cellulose nanofiber scaffold composites. *Int J Biol Macromol*. 2022;223:479–89.
172. Hong FF. A biodegradable antibacterial nanocomposite based on oxidized bacterial nanocellulose for rapid hemostasis and wound healing. *ACS Appl Mater Interfaces*. 2020;12:3382–92.
173. Torgbo S, Sukyai P. Biodegradation and thermal stability of bacterial cellulose as biomaterial: The relevance in biomedical applications. *Polym Degrad Stab* 2020;179:109232.
174. Tamo AK, Tran TA, Doench I, Jahangir S, Lall A, David L, et al. 3D printing of cellulase-laden cellulose nanofiber/chitosan hydrogel composites: towards tissue engineering functional biomaterials with enzyme-mediated biodegradation. *Materials (Basel)*. 2022;15:6039.
175. Norizan MN, Moklis MH, Demon SZN, Halim NA, Samsuri A, Mohamad IS, et al. Carbon nanotubes: functionalization and their application in chemical sensors. *RCS Adv*. 2020;10:43704–32.

**Publisher's Note** Springer Nature remains neutral with regard to jurisdictional claims in published maps and institutional affiliations.

Springer Nature or its licensor (e.g. a society or other partner) holds exclusive rights to this article under a publishing agreement with the author(s) or other rightsholder(s); author self-archiving of the accepted manuscript version of this article is solely governed by the terms of such publishing agreement and applicable law.